6th Summer School in Analysis and Applied Mathematics
Rome 20-24 June 2011

Modeling and Complexity Reduction in PDES for Multiphysics

Modeling the Circulatory System

Alfio Quarteroni

EPFL, Lausanne (Switzerland)
MATHICSE Mathematics Institute of Computational Science and Engineering

POLITECNICO di MILANO (Italy)
MOX Modellistica e Calcolo Scientifico

The Context

1. From clinical imaging to computational grid

2. Mathematical Modeling

3. Computing

4. Verification Validation

5. Clinical Applications

From Images to Grid

Image Processing and Volume Reconstruction

3D Magnetic Resonance Imaging (MRI) data: patient anatomical information

Vessel's (lumen) extraction via *level set segmentation* (VMTK)

Mesh generation (Netgen) for fluid-dynamics simulations

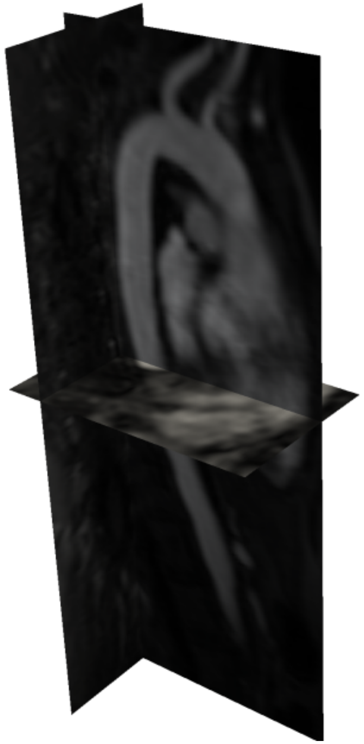

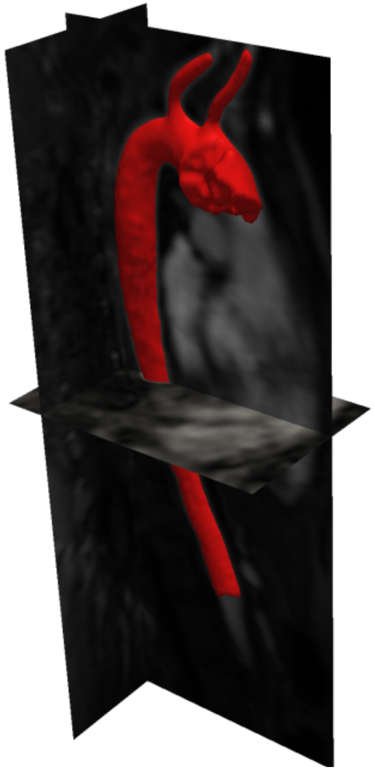

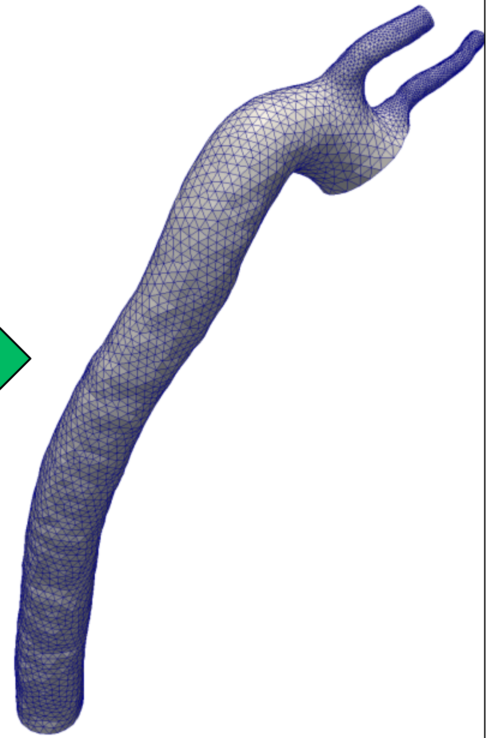

This "snapshot" has been obtained as an average over the cardiac cycle that could be considered as the diastolic configuration

Aortic arch (courtesy of MD Luciani and MD Puppini, Ospedale Borgo Trento, Verona, Italy)
(E.Faggiano, G.B.Luciani, G.Puppini, C.Vergara, 2010)

Image Processing (cont'd) 4D Displacement Data

AAA - Aneurysm in the Abdominal Aorta

4D MRI data: anatomical information of the patient at 10-20 instants over the cardiac cycle

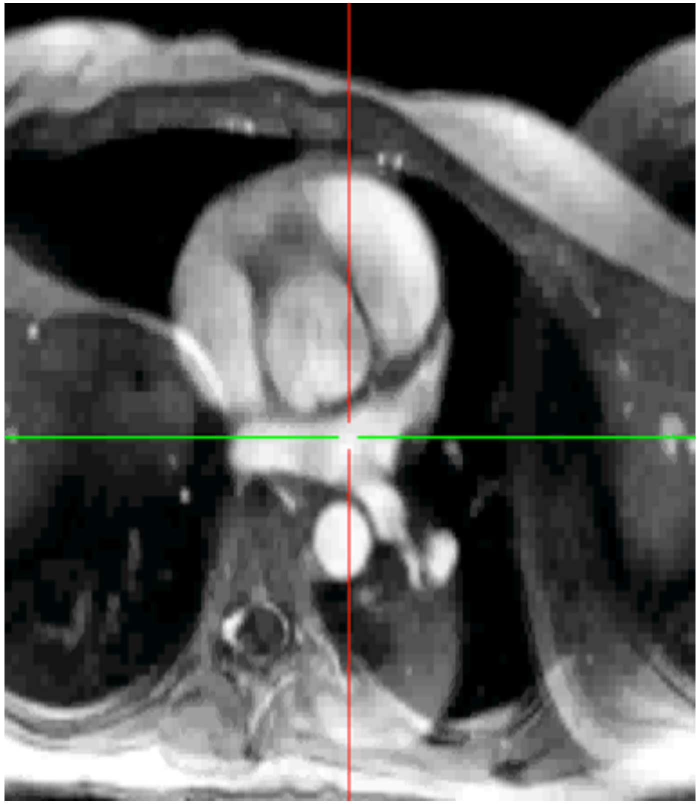

Vessel segmentation and surface registration → displacement analysis (VMTK)

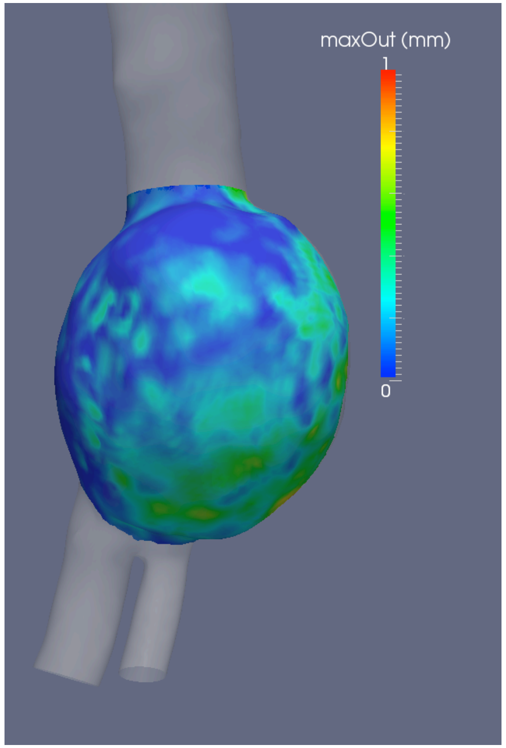

Normalized maximum (in time) displacement with respect to the diastolic configuration

Aortic arch, courtesy of MD M. Domanin, Policlinico di Milano, Italy

AAA - Aneurysm in the Abdominal Aorta

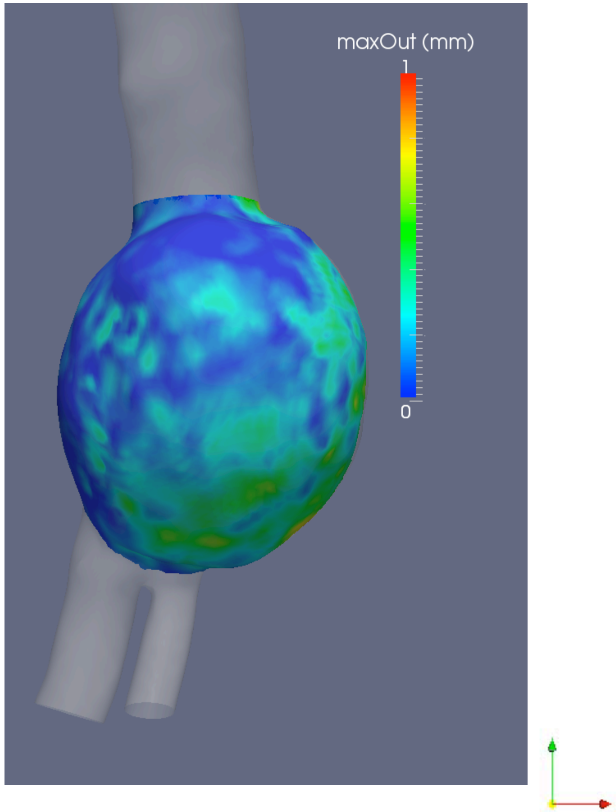

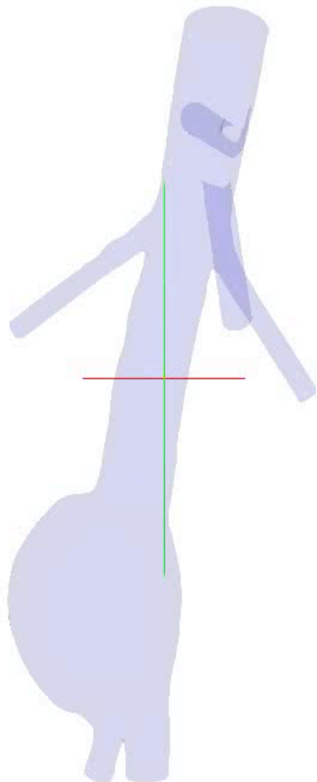

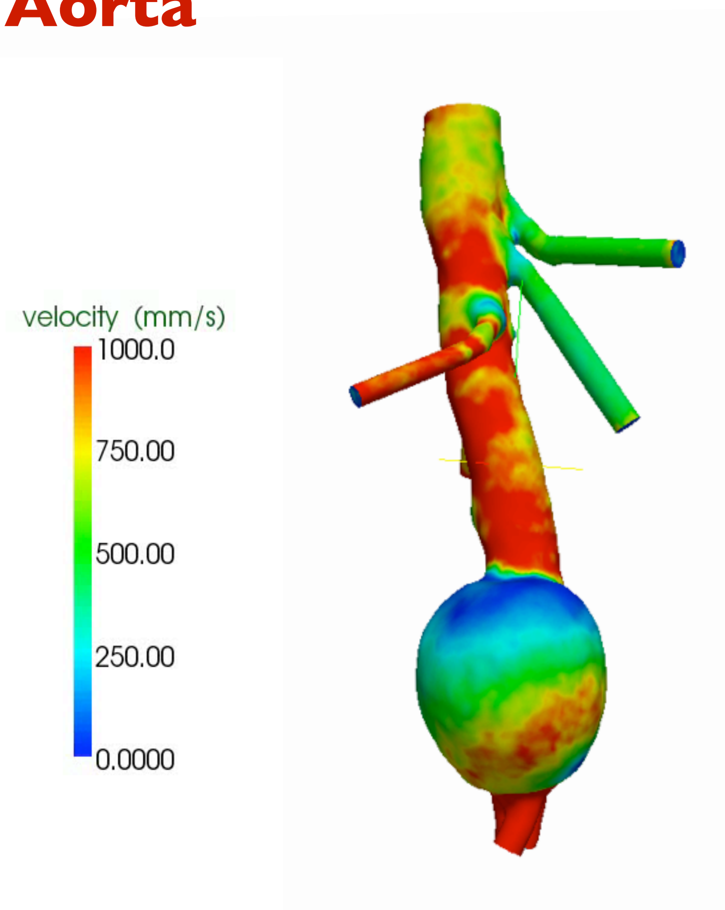

Normalized maximum (in time) displacement with respect to the diastolic configuration

The zone of highest jet's incidence is the one of maximum displacement on the figure on the left

Numerical simulation (LIFEV): blood velocity pattern and WESS (Courtesy: M.Piccinelli and C.Vergara)

Importance of grid quality: FSI simulation in a femoral bypass

Patient-specific geometry and boundary conditions

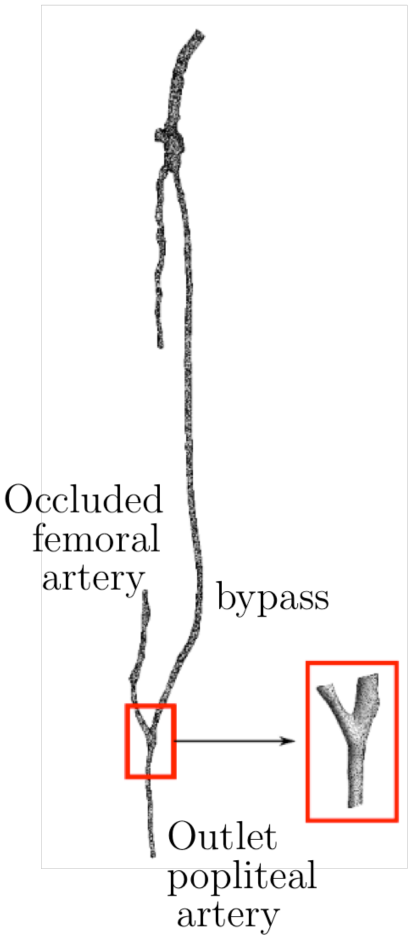

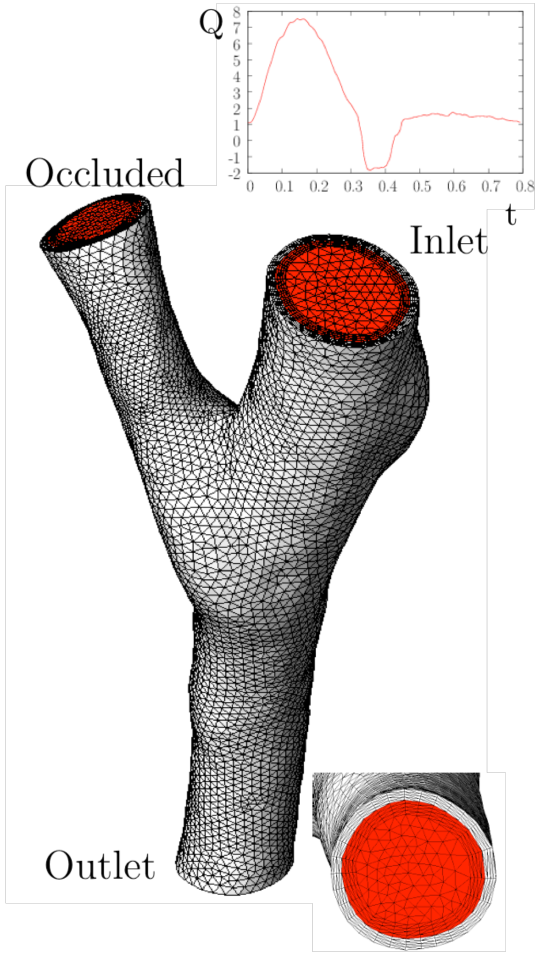

With boundary layer

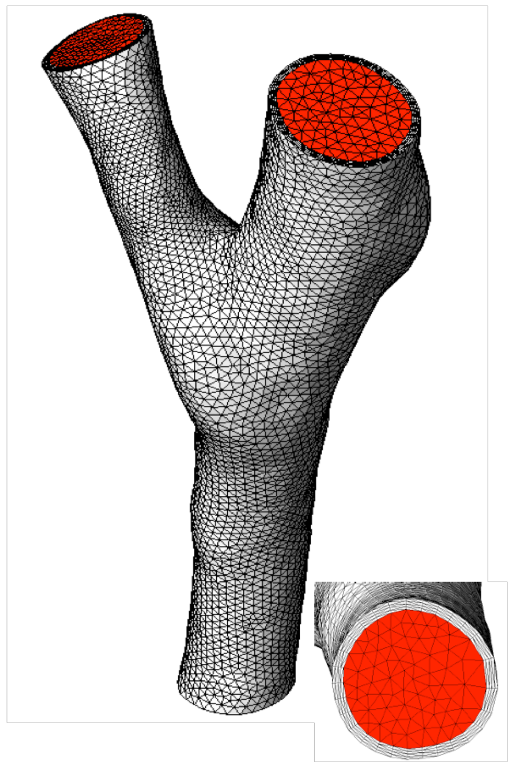

Without boundary layer

Numerical simulation: Marchandise, Crosetto, Geuzaine, Remacle, Sauvage, 2010

FSI in a femoral bypass

Influence of boundary layer grid on wall shear stress (WSS)

Three different grids, meshes with and without BL

Boundary layer grids

Grids without boundary layer

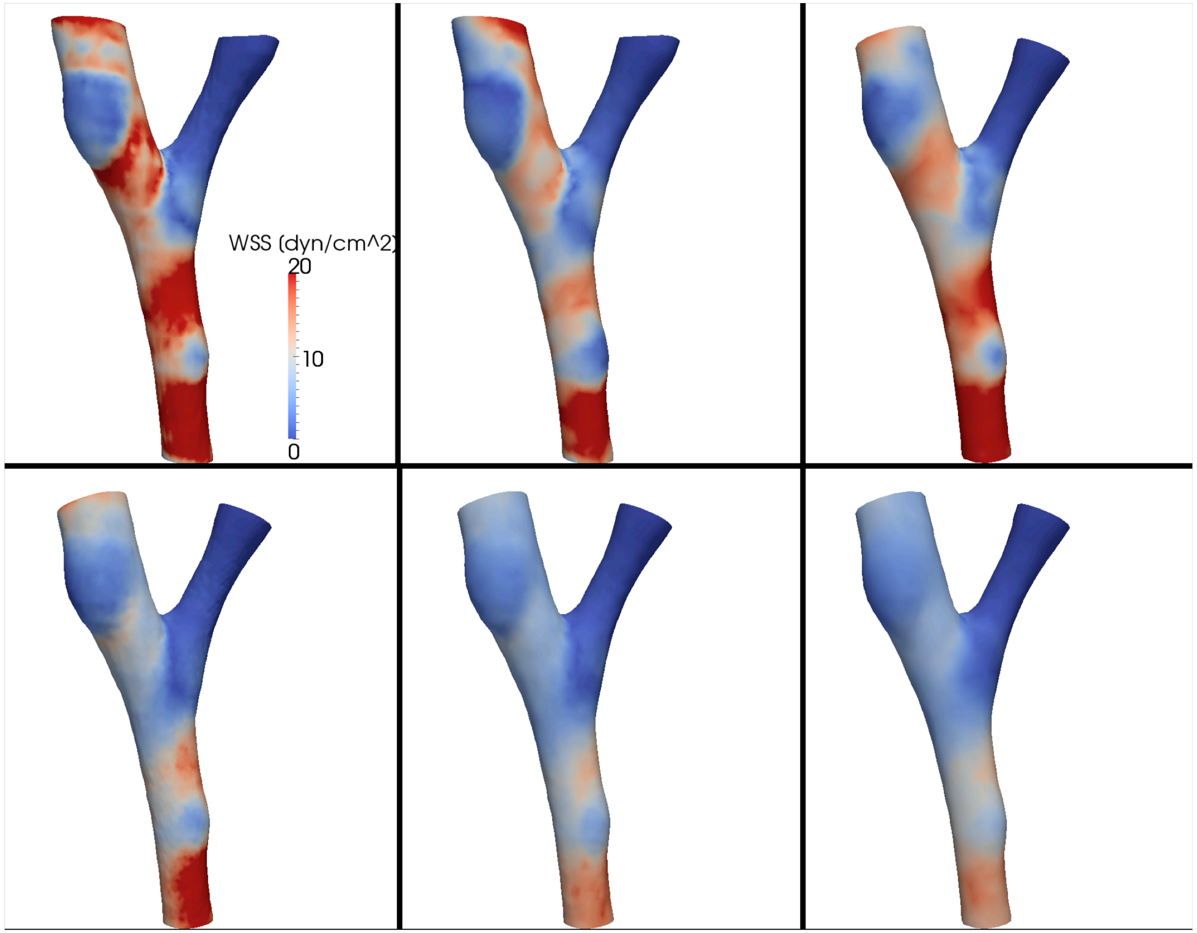

All three meshes without boundary layer (lower) fail to capture the correct WSS.
Fluid meshes ranging from 9,000 to 213,000 nodes

Modeling

Local flow analysis - Incompressible Newtonian Flow

- Navier-Stokes equations in carotid artery with rigid walls
- Pulsatile inflow - defective b.c at outflow

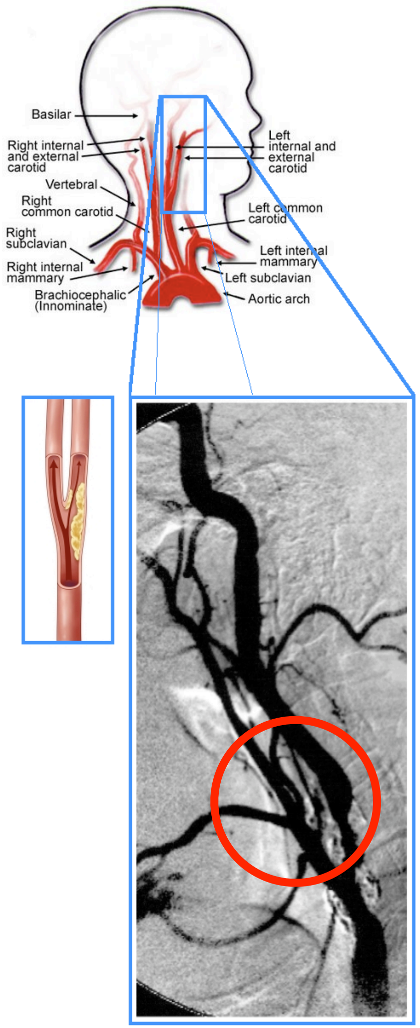

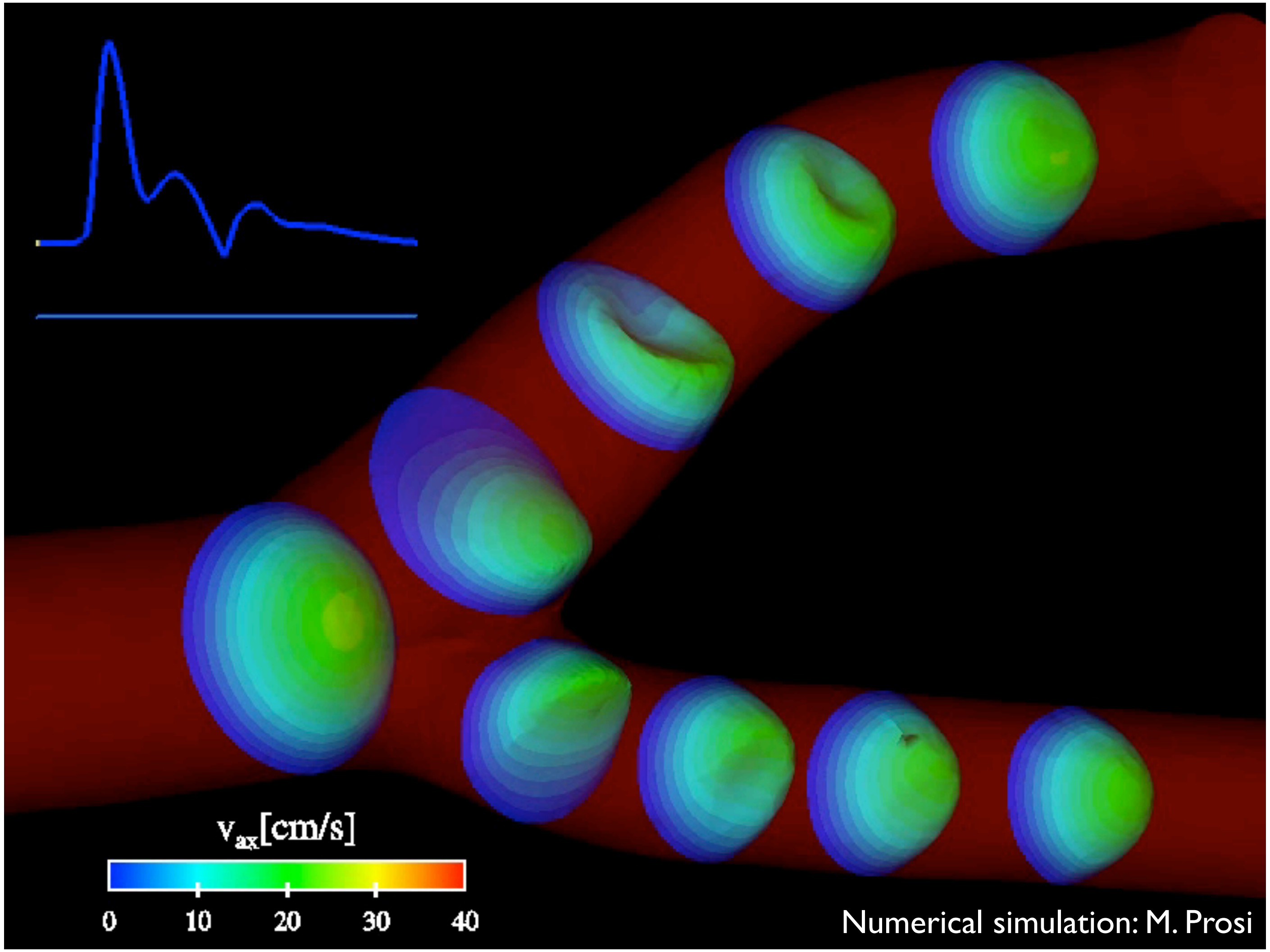

Modeling:

Vessel Compliance

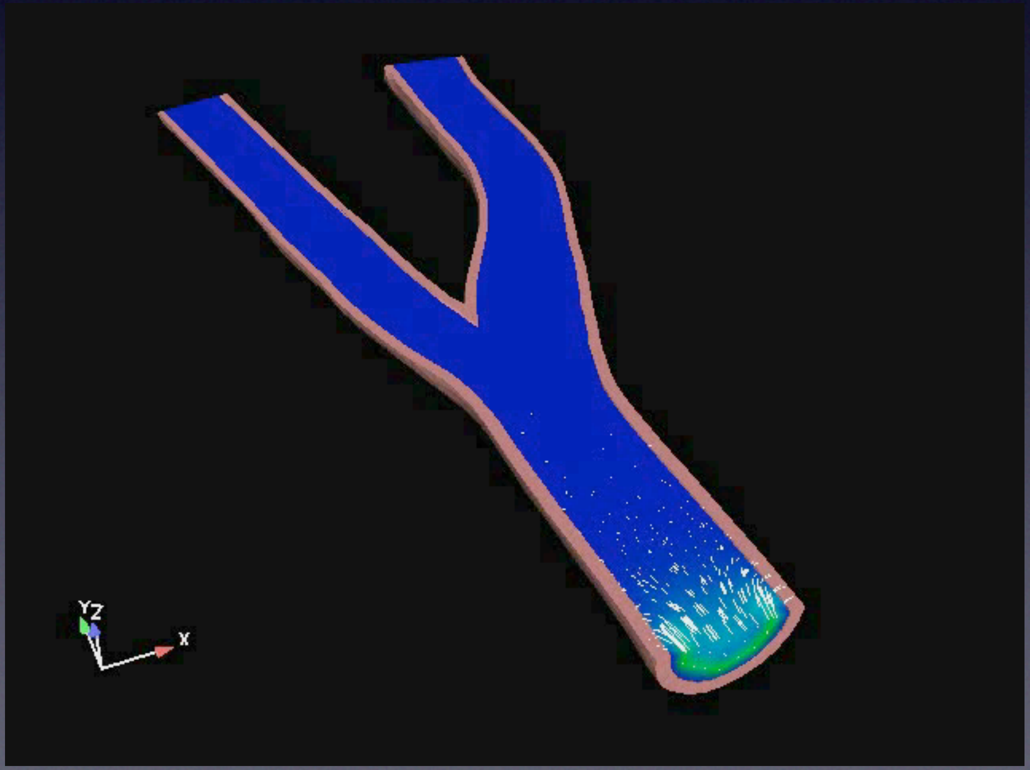

Abstract setting - FSI: the ALE frame of reference

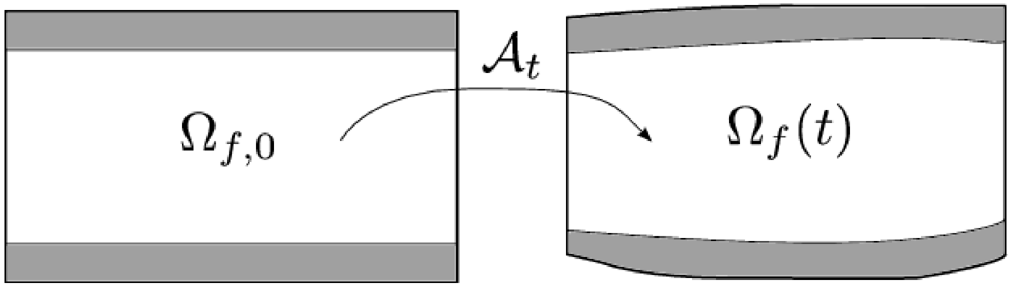

- ***ALE mapping***

  The computational domain Ω in the Eulerian formulation. It is a fixed portion of space filled by the medium during its motion

- ***ALE derivative***

$$\left.\frac{\partial q}{\partial t}\right|_{\widetilde{\mathcal{A}}} = \mathbf{w} \cdot \nabla q + \frac{\partial q}{\partial t}$$

The moving grid and the ALE velocity

A coupled fluid-structure problem

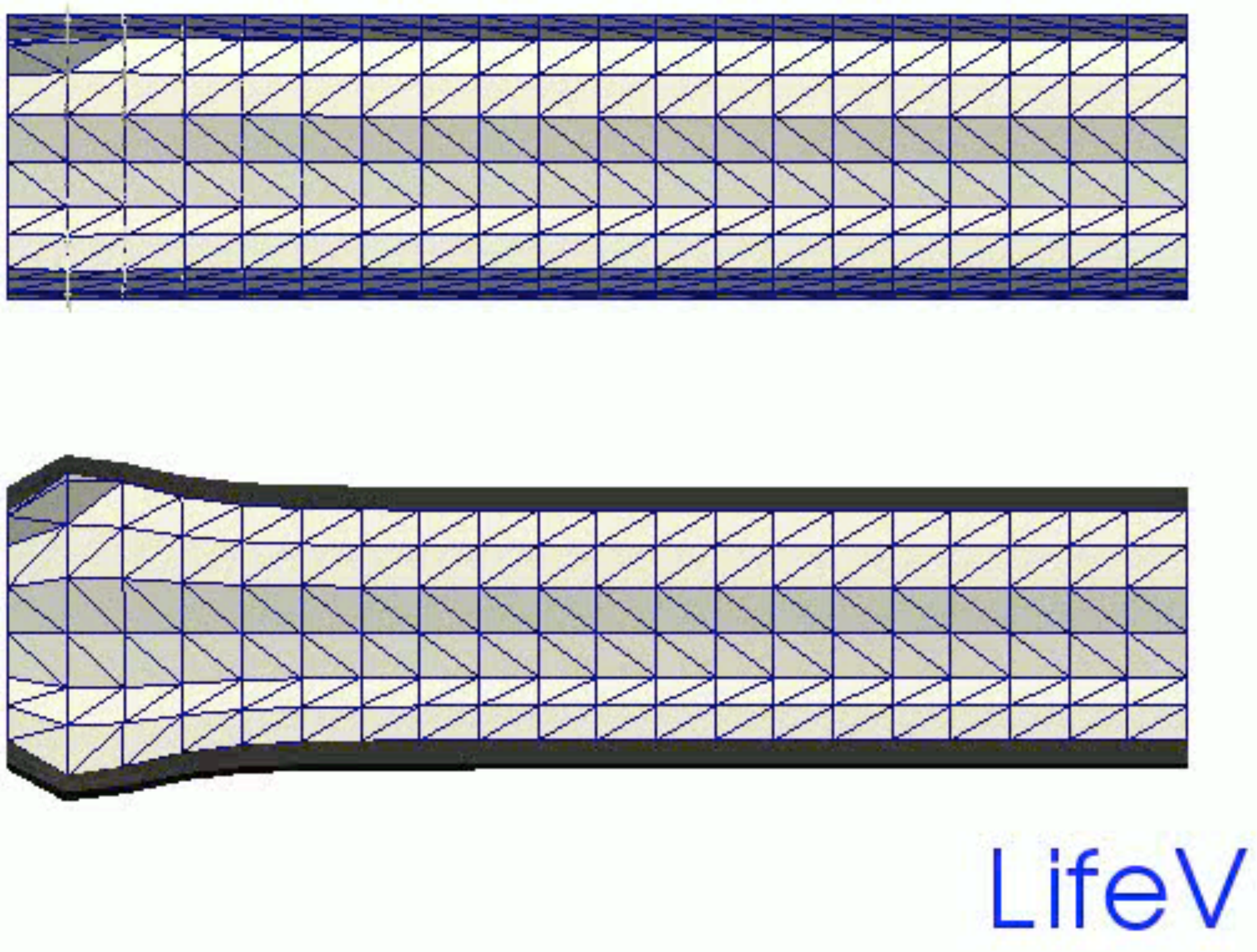

The Reynolds transport theorem

Let $\widetilde{\omega}_0 \subset \widetilde{\omega}$ *be a subdomain in the ALE reference configuration and* $\omega_0(t) = \widetilde{\mathcal{A}}(\widetilde{\omega}_0, t) \subset \omega(t)$ *it image by the ALE map. Then for any continuously differentiable field:*

$$\frac{\mathrm{d}}{\mathrm{d}\,t} \int_{\omega_0(t)} f \,\mathrm{d}\mathbf{x} = \int_{\omega_0(t)} \left(\left.\frac{\partial f}{\partial t}\right|_{\widetilde{\mathcal{A}}} + f \,\mathrm{div}\, \boldsymbol{w} \right) \mathrm{d}\mathbf{x}$$

$$= \int_{\omega_0(t)} \left(\frac{\partial f}{\partial t} + \mathrm{div}\,(f \boldsymbol{w}) \right) \mathrm{d}\mathbf{x}$$

A coupled fluid-structure problem

Equations for the geometry:

$$\hat{\eta}_f = \mathrm{Ext}(\hat{\eta}_{s|\hat{\Gamma}}), \; \hat{\mathbf{w}} = \frac{\partial \hat{\eta}_f}{\partial t}, \Omega_f(t) = (I + \hat{\eta}_f)(\hat{\Omega}_f)$$

Equations for the fluid:

$$\frac{\rho_f}{J_{\hat{\mathcal{A}}}} \frac{\partial J_{\hat{\mathcal{A}}} \mathbf{u}_f}{\partial t}_{|\hat{\mathbf{x}}} + \mathrm{div}(\rho_f \mathbf{u}_f \otimes (\mathbf{u}_f - \mathbf{w}) - \sigma_f(\mathbf{u}_f, P)) = 0, \quad \text{in} \quad \Omega_f(t)$$

$$\mathrm{div}\mathbf{u}_f = 0, \quad \text{in} \quad \Omega_f(t)$$

$$\mathbf{u}_f = \mathbf{u}_D, \quad \text{on} \quad \Gamma_{f,D}$$

$$\sigma_f(\mathbf{u}_f, P)\mathbf{n}_f = \mathbf{g}_{f,N}, \quad \text{on} \quad \Gamma_{f,N}$$

$$\mathbf{u}_f = \mathbf{w}, \quad \text{on} \quad \Gamma(t)$$

Equations for the structure:

$$\hat{\rho}_{s,0} \frac{\partial^2 \hat{\eta}_s}{\partial t^2} - \mathrm{div}_{\hat{\mathbf{x}}}(\hat{\mathbf{F}}_s \hat{\Sigma}) = 0, \quad \text{in} \quad \hat{\Omega}_s$$

$$\hat{\eta}_s = 0 \quad \text{on} \quad \hat{\Gamma}_{s,D}$$

$$\hat{\mathbf{F}}_s \hat{\Sigma} \hat{\mathbf{n}}_s = \hat{J}_s |\hat{\mathbf{F}}_s^{-T} \hat{\mathbf{n}}_s| \hat{\mathbf{g}}_{s,N}, \quad \text{on} \quad \hat{\Gamma}_{s,N}$$

$$\hat{\mathbf{F}}_s \hat{\Sigma} \hat{\mathbf{n}}_s = \hat{J}_s \hat{\sigma}_f(\mathbf{u}_f, P) \hat{\mathbf{F}}_s^{-T} \hat{\mathbf{n}}_s, \quad \text{on} \quad \hat{\Gamma}$$

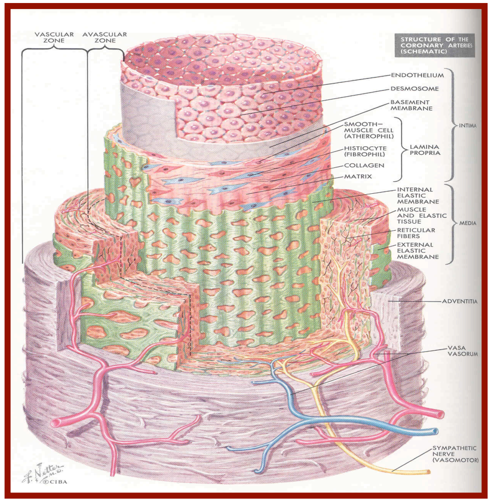

Surface registration

Surface registration:

find the alignment of the surfaces of two consecutive time frames

- construction of a **displacement field** η_{meas} which maps the surface points

Surface registration could be used to solve a FSI problem **without solving the structure:**

- Solve the **ALE fluid problem** in a moving domain with known boundary

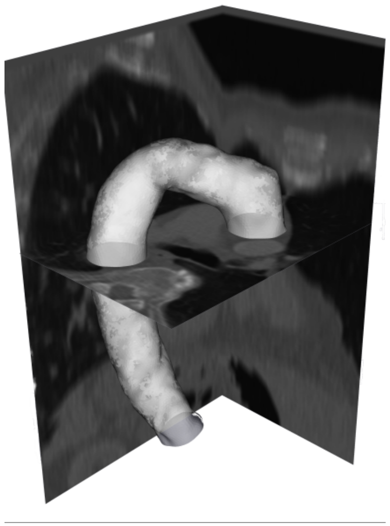

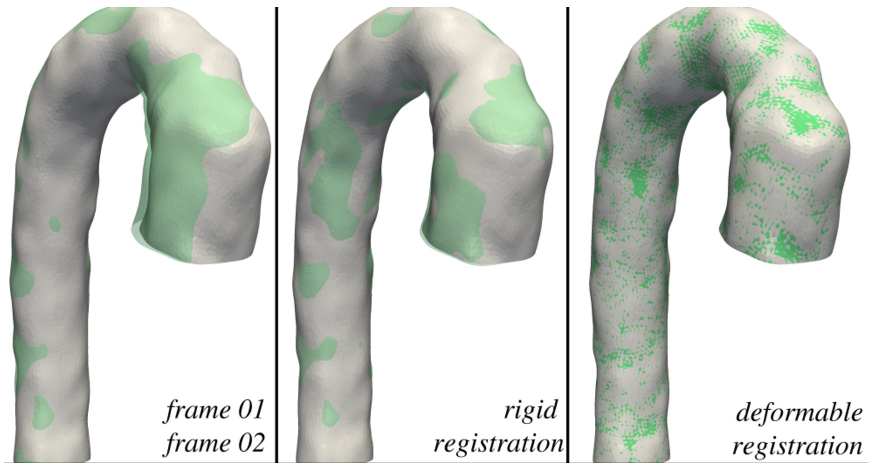

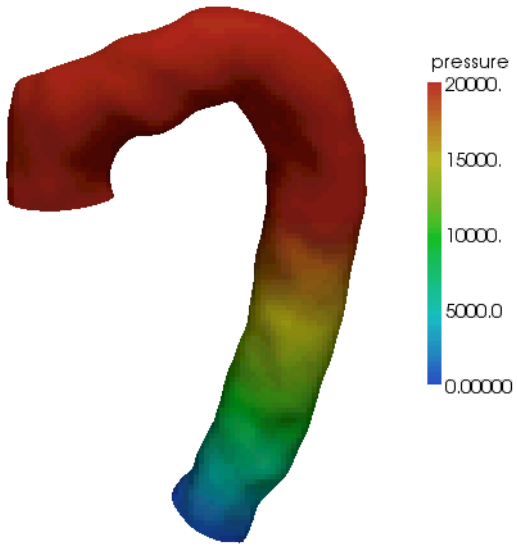

Acknowledgement: A. Veneziani, M.Piccinelli, L. Mirabella, T.Passerini

(Variational) data assimilation

I) Based on surface registration

Example: determine the rigidity of a vessel

Find the minimum of

$$\mathcal{J} = \int_{\Sigma} \left(\boldsymbol{\eta}_{meas}(\boldsymbol{x}, \tau_k) - \boldsymbol{\eta}(\boldsymbol{x}, \tau_k)\right)^2 d\sigma.$$

under the constraint given by the **FSI** problem

II) Based on volumetric data

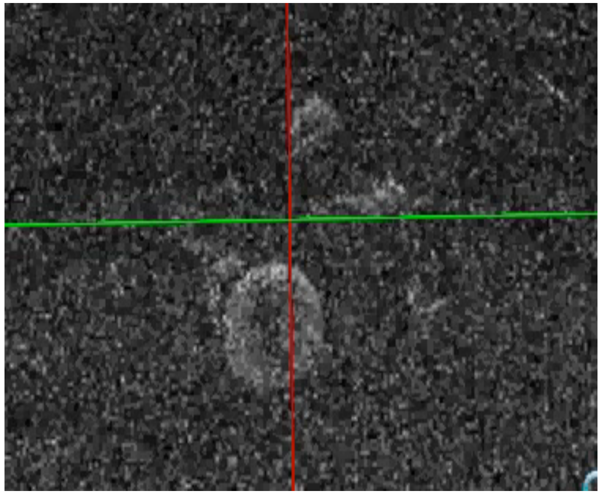

4D Phase-contrast MRI data: blood velocity at specific slices at 10-20 instants over the cardiac cycle

Velocity vectors extraction

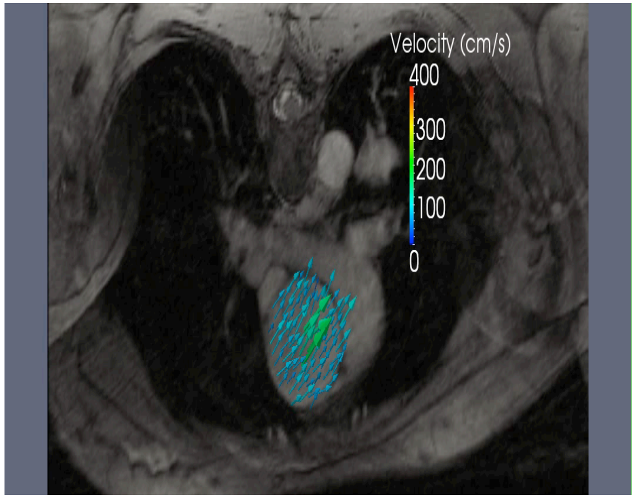

(M.Perego, A.Veneziani, C.Vergara,
A variational approach for estimating the compliance of the cardiovascular tissue, SIAM J Sci Comp, 2011)

(M.D'Elia. PhD Thesis, Emory University)

Computing -
Complexity

Geometric Multiscaling

Global Flow Analysis: System's Complexity

- **Morphological complexity**: the diameter of blood vessels ranges from 10^{-2} m down to 10^{-6} m. Consequently, the flow regime varies considerably.

Vessel	Radius(cm)	Number	Reynolds number
Aorta	**1.25**	**1**	**3400**
Arteries	**0.2**	**159**	**55**
Arterioles	**1.5×10^{-3}**	**5.7×10^{7}**	**0.7**
Capillaries	**3×10^{-4}**	**1.6×10^{10}**	**0.002**
Venules	**1×10^{-3}**	**1.3×10^{9}**	**0.01**
Veins	**0.25**	**200**	**140**
Vena cava	**1.5**	**1**	**3300**

- **Functional complexity**: the cardiovascular system is able to react to changes in the external environment and presents several 'non-linear' components (e.g. valves). We need to account for the local/systemic interactions.

Geometric multiscaling in the circulatory system

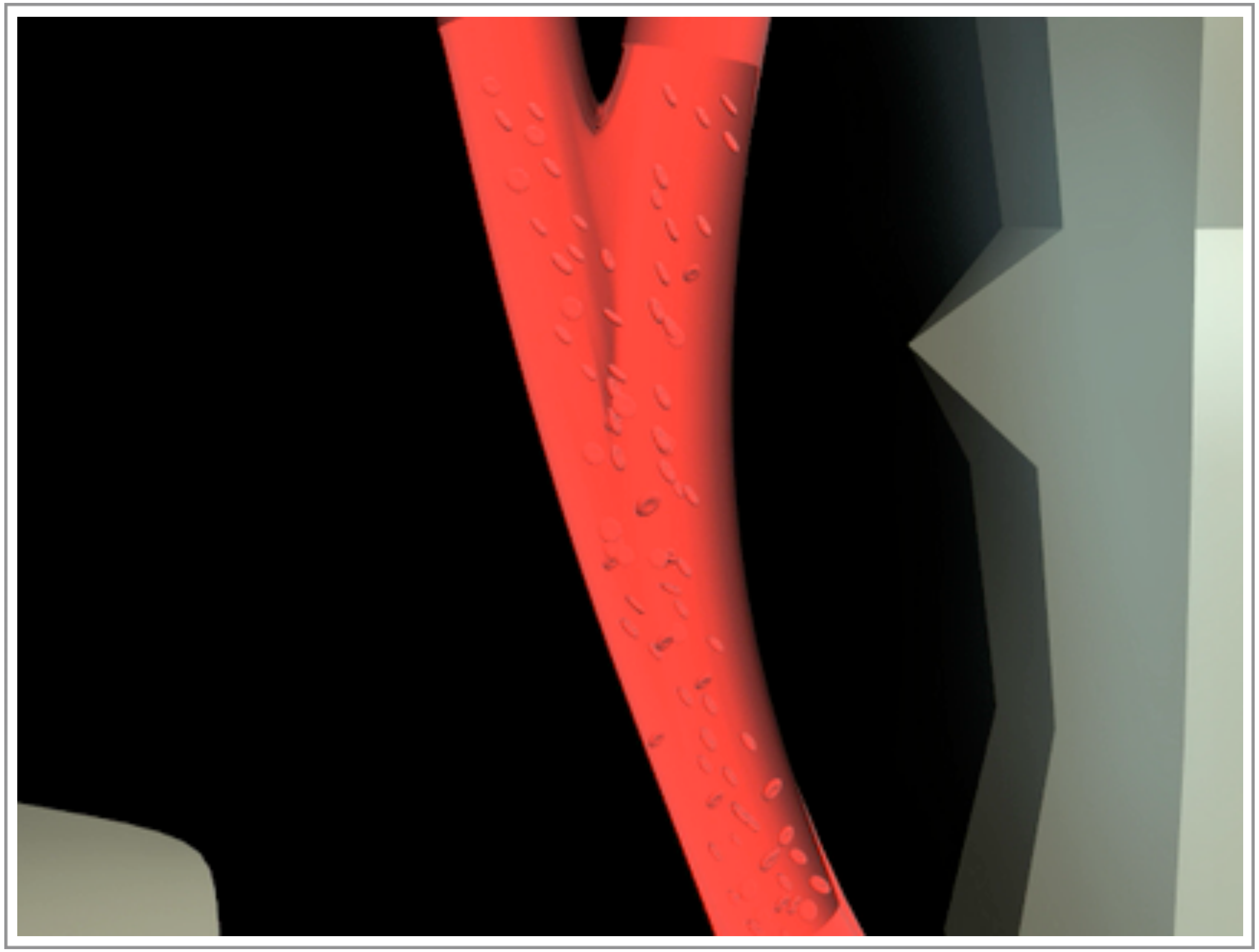

Local: 3D FSI flow model

Global: 1D network of arteries and veins (Euler hyperbolic system)

Global: 0D capillary network (DAE system)

Geometric multiscaling in the circulatory system

3*D*

1*D*

0*D*

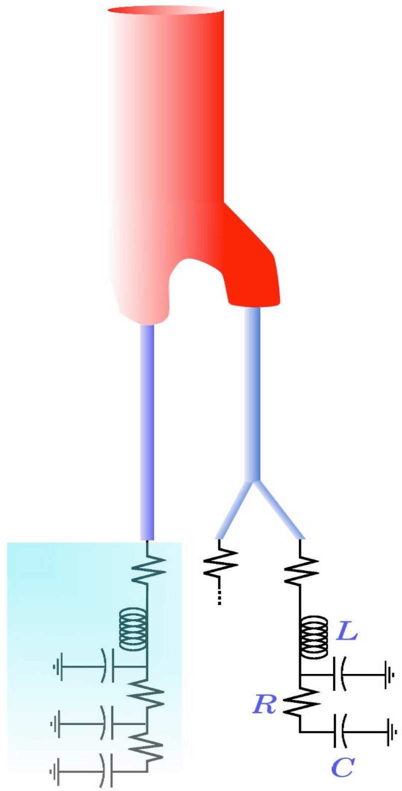

3D Navier-Stokes (F)
+
3D ElastoDynamics (V-W)

1D Euler (F)
+
Algebraic pressure law

0D lumped parameters
(system of linear ODEs)

(L. Formaggia, A.Q, A. Veneziani: Cardiovascular Mathematics, Springer, 2009)

3D

3D Navier-Stokes (F) + 3D ElastoDynamics (V-W)

$$\frac{\rho_f}{J_{\hat{A}}}\frac{\partial J_{\hat{A}}\mathbf{u}_f}{\partial t}\Big|_{\hat{\mathbf{x}}} + \mathrm{div}(\rho_f \mathbf{u}_f \otimes (\mathbf{u}_f - \mathbf{w}) - \sigma_f(\mathbf{u}_f, P)) = 0, \quad \text{in } \Omega_f(t)$$
$$\mathrm{div}\,\mathbf{u}_f = 0, \quad \text{in } \Omega_f(t)$$
$$\mathbf{u}_f = \mathbf{u}_D, \quad \text{on } \Gamma_{f,D}$$
$$\sigma_f(\mathbf{u}_f, P)\mathbf{n}_f = \mathbf{g}_{f,N}, \quad \text{on } \Gamma_{f,N}$$
$$\mathbf{u}_f = \mathbf{w}, \quad \text{on } \Gamma(t)$$

$$\hat{\rho}_{s,0}\frac{\partial^2 \hat{\eta}_s}{\partial t^2} - \mathrm{div}_{\hat{\mathbf{x}}}(\hat{\mathbf{F}}_s \hat{\Sigma}) = 0, \quad \text{in } \hat{\Omega}_s$$
$$\hat{\eta}_s = 0 \quad \text{on } \hat{\Gamma}_{s,D}$$
$$\hat{\mathbf{F}}_s \hat{\Sigma} \hat{\mathbf{n}}_s = \hat{J}_s |\hat{\mathbf{F}}_s^{-T} \hat{\mathbf{n}}_s| \hat{\mathbf{g}}_{s,N}, \quad \text{on } \hat{\Gamma}_{s,N}$$
$$\hat{\mathbf{F}}_s \hat{\Sigma} \hat{\mathbf{n}}_s = \hat{J}_s \hat{\sigma}_f(\mathbf{u}_f, P)\hat{\mathbf{F}}_s^{-T}\hat{\mathbf{n}}_s, \quad \text{on } \hat{\Gamma}$$

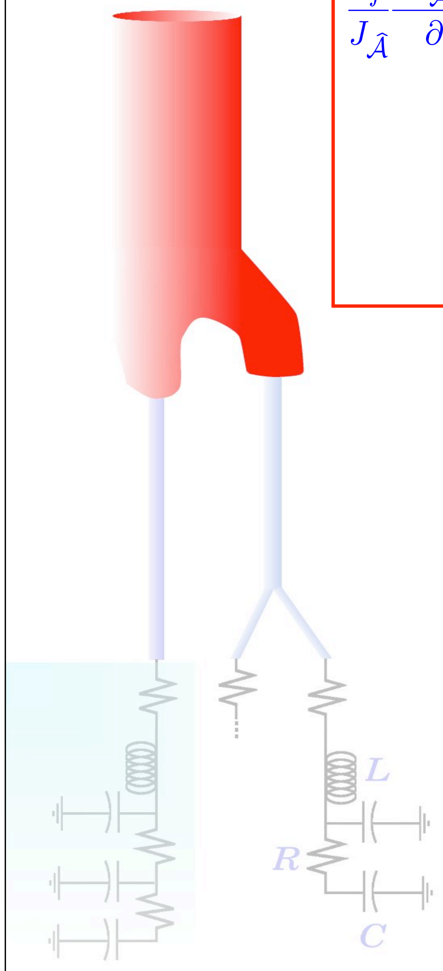

Assume to:

- $u_z >> u_x, u_y$
- u_z has a prescribed steady profile
- average over axial sections
- static equilibrium for the vessel

Then we obtain a 1D problem

1D

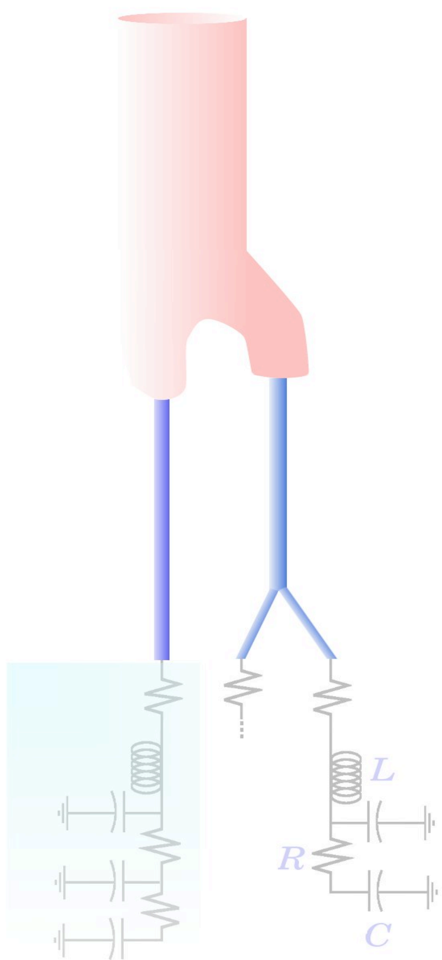

1D Euler(F) + Algebraic pressure law

$$\begin{aligned} \partial_t A + \partial_x Q &= 0, \\ \partial_t Q + \partial_x \left(\frac{\alpha Q}{A}\right) + \frac{A}{\rho}\partial_x P &= -K_r \frac{Q}{A}, \\ P(A) &= \beta \frac{\sqrt(A) - \sqrt(A_0)}{A_0} \end{aligned}$$

Assume to:

- linearize 1D equations
- consider average internal variables
- relate interface values to averaged ones

Then we obtain a 0D problem (ODE)

Mathematical Model

0*D*

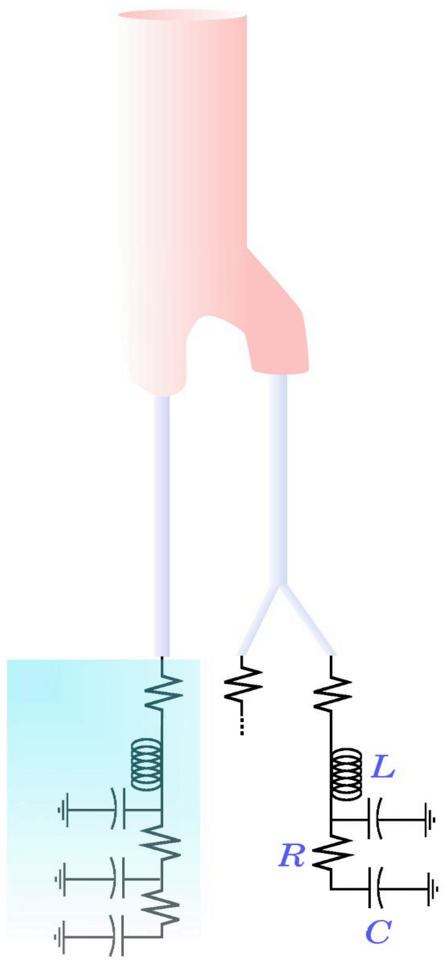

0D Lumped parameters (system of linear ODE's)

$$C\frac{dP_i}{dt} = -(Q_{i+1} - Q_i),$$

$$L\frac{dQ_i}{dt} = -(P_i - P_{i-1}) - RQ_i$$

Fluid dynamics	Electrical circuits
Pressure	Voltage
Flow rate	Current
Blood viscosity	Resistance R
Blood inertia	Inductance L
Wall compliance	Capacitance C

- RLC circuits model "large" arteries
- RC circuits account for capillary bed
- Can describe compartments (such as peripheral circulation)

The 1D Network

At a bifurcation we prescribe

✓ Continuity of total pressure: $p_{t,1} = p_{t,2} = p_{t,3}$

✓ Conservation of mass: $\Sigma_i \, Q_i = 0$

Mathematical Analysis

The coupled problem satisfies a stability estimate similar to that of the single artery model.
No shock waves developing, explicit form of characteristic variables available

In principle, it is possible to *account for curvature, tapering, and for the bifurcation angle* through an energy loss term.

In practice, this has a minor impact on numerical results

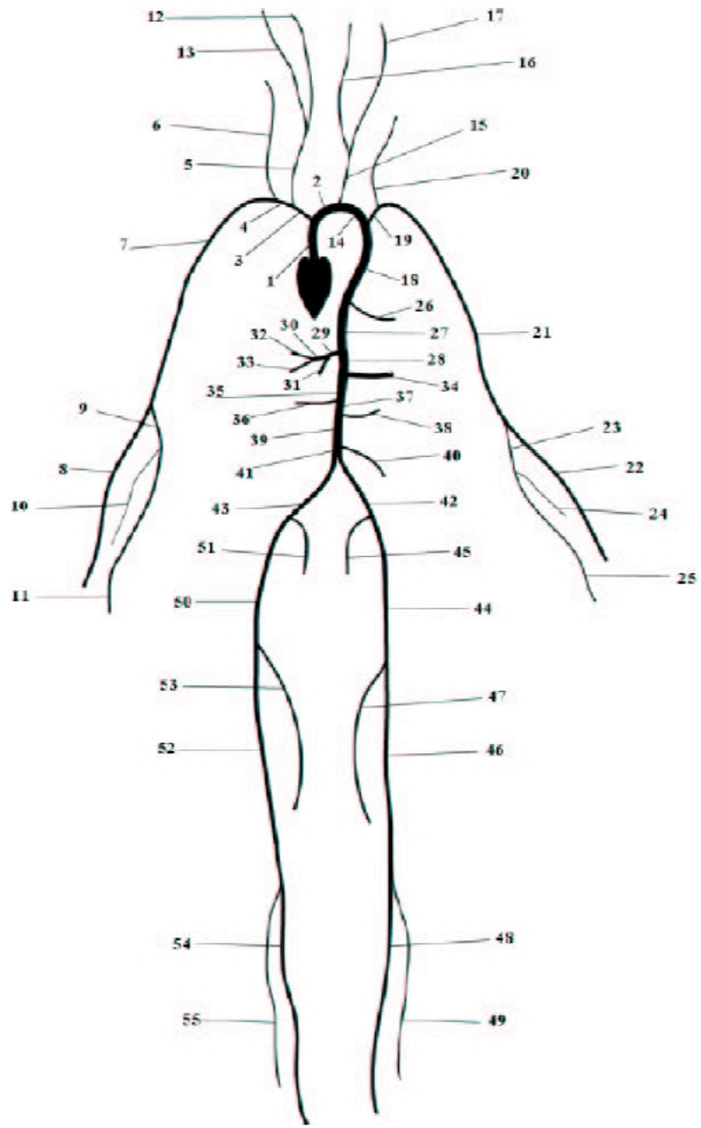


Peripheral branches:
Absorbing b.c
Colormap: A/A0-1
LifeV
Cristiano Malossi @ CMCS
LifeV
Cristiano Malossi @ CMCS

1D model of circulation: peripheral resistance

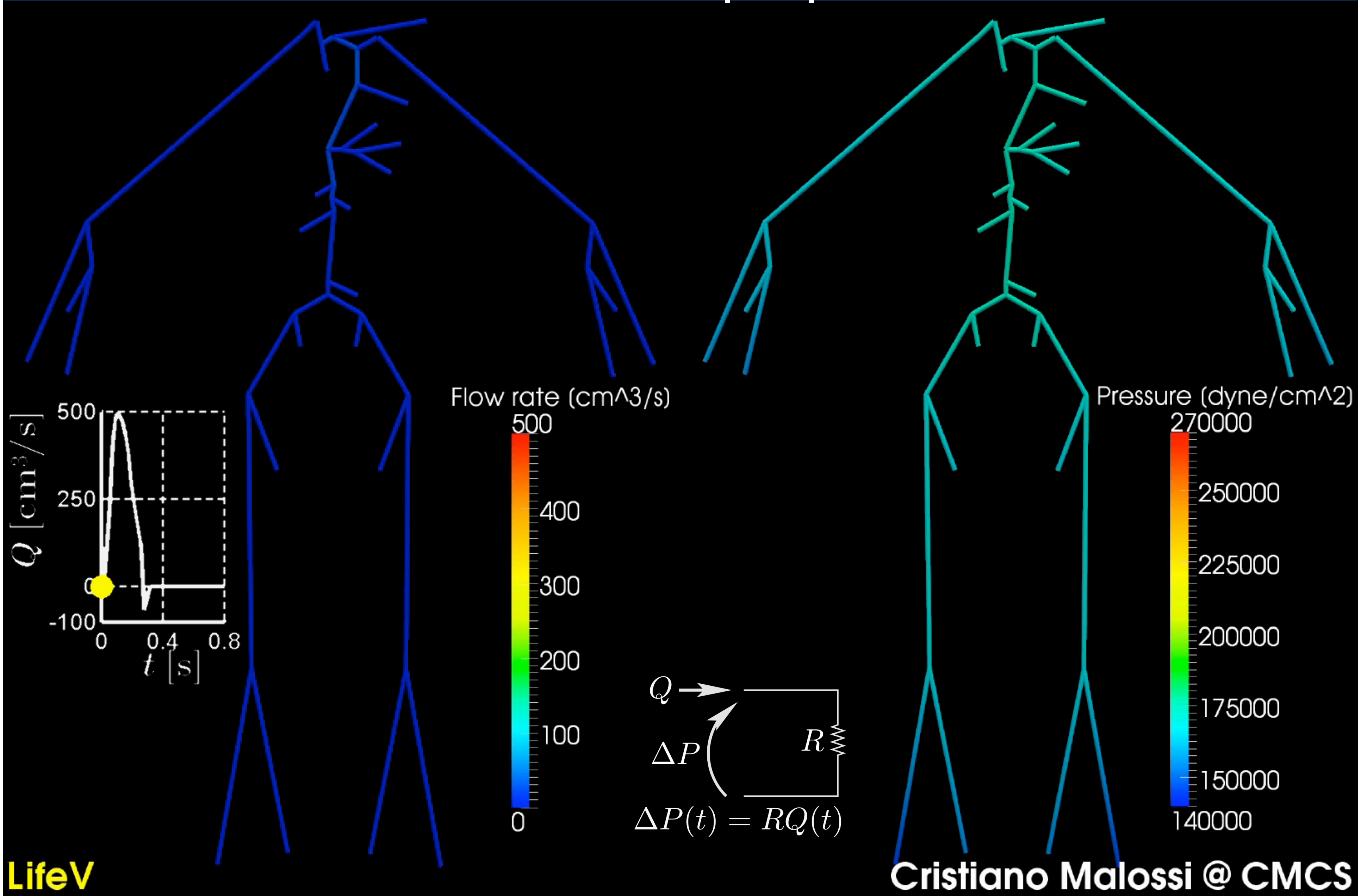

3D-1D for the carotid artery: pressure pulse

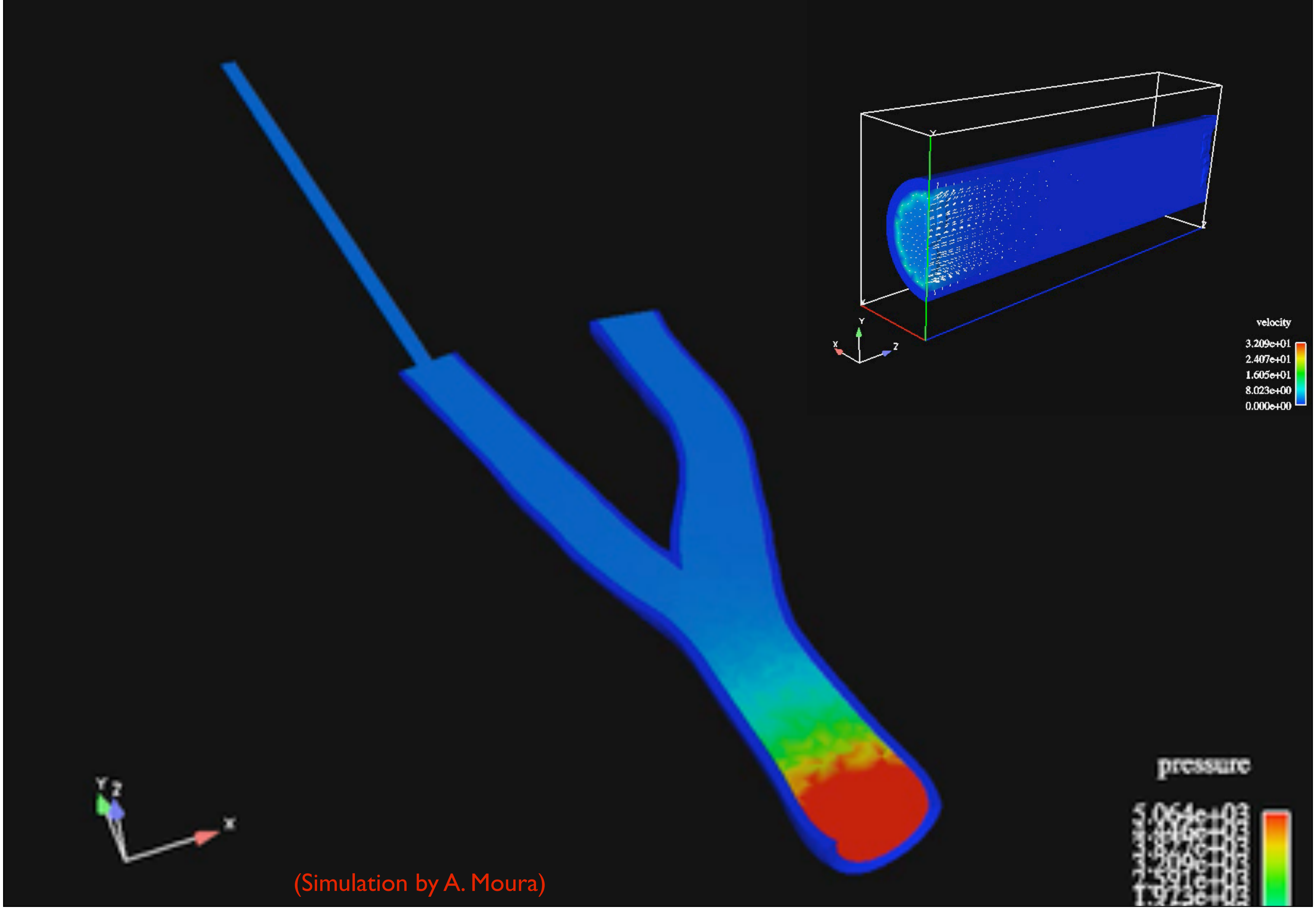

(Simulation by A. Moura)

Geometric Multiscale - an Instance

Models:

- 3-D FSI Aorta & Iliac Artery
- 1-D arterial tree
  - 92 tapered elements
  - viscoelastic wall
- 0-D terminals
  - 47 Windkessel elements (RCR)

Coupling:

- averaged/integrated quantities at the interfaces (flow rate or normal stress)
- segregated approach for the solution of the coupled problem (Newton, inexact-Newton, or Broyden methods)

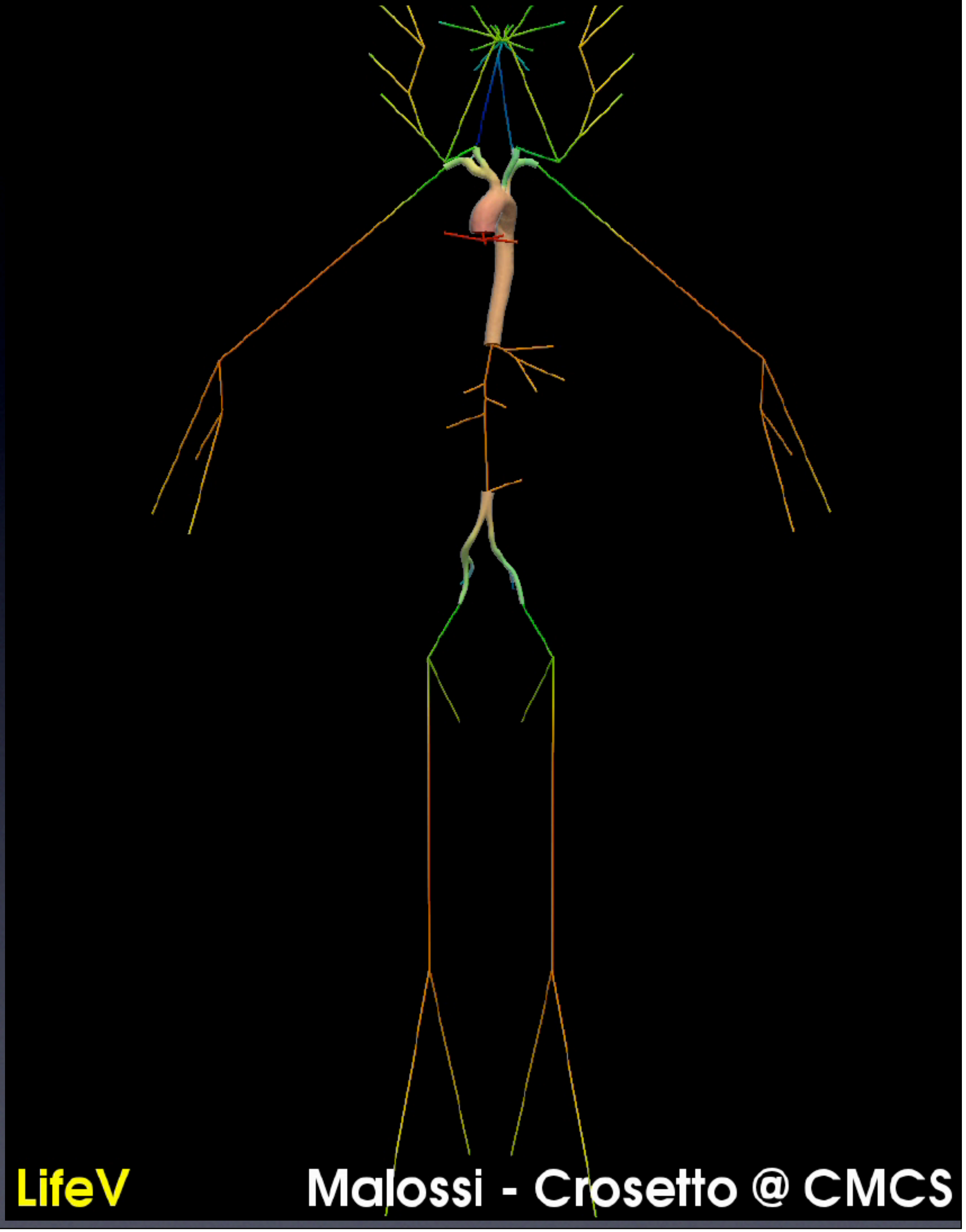

Imbedded 1D-3D

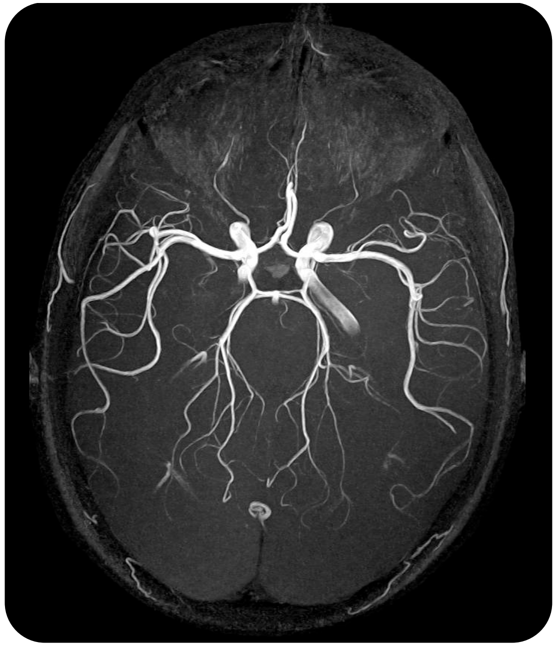

Application to oxygen transport in the brain: *isosurface of oxygen concentration.*

Impairment due to left carotid artery occlusion.

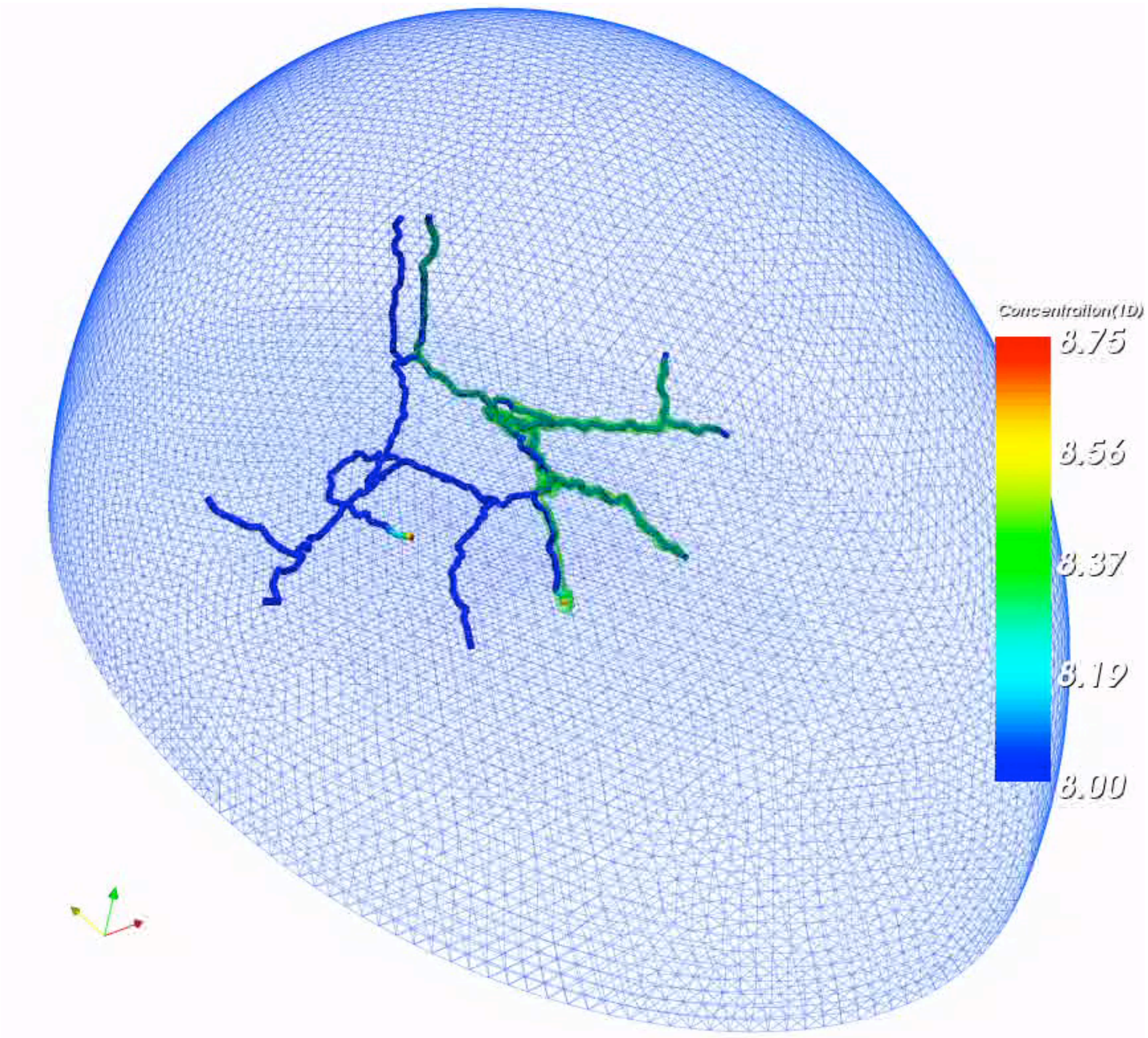

(Simulations by C. D'Angelo)

Blood Flow and Oxygen Transport in the Brain

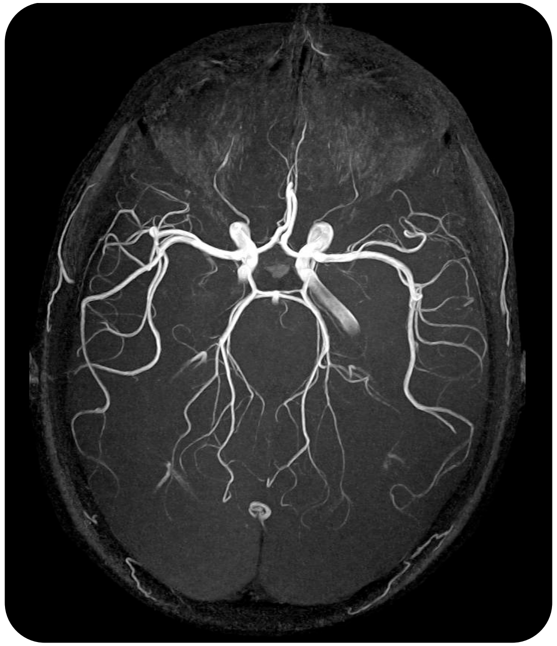

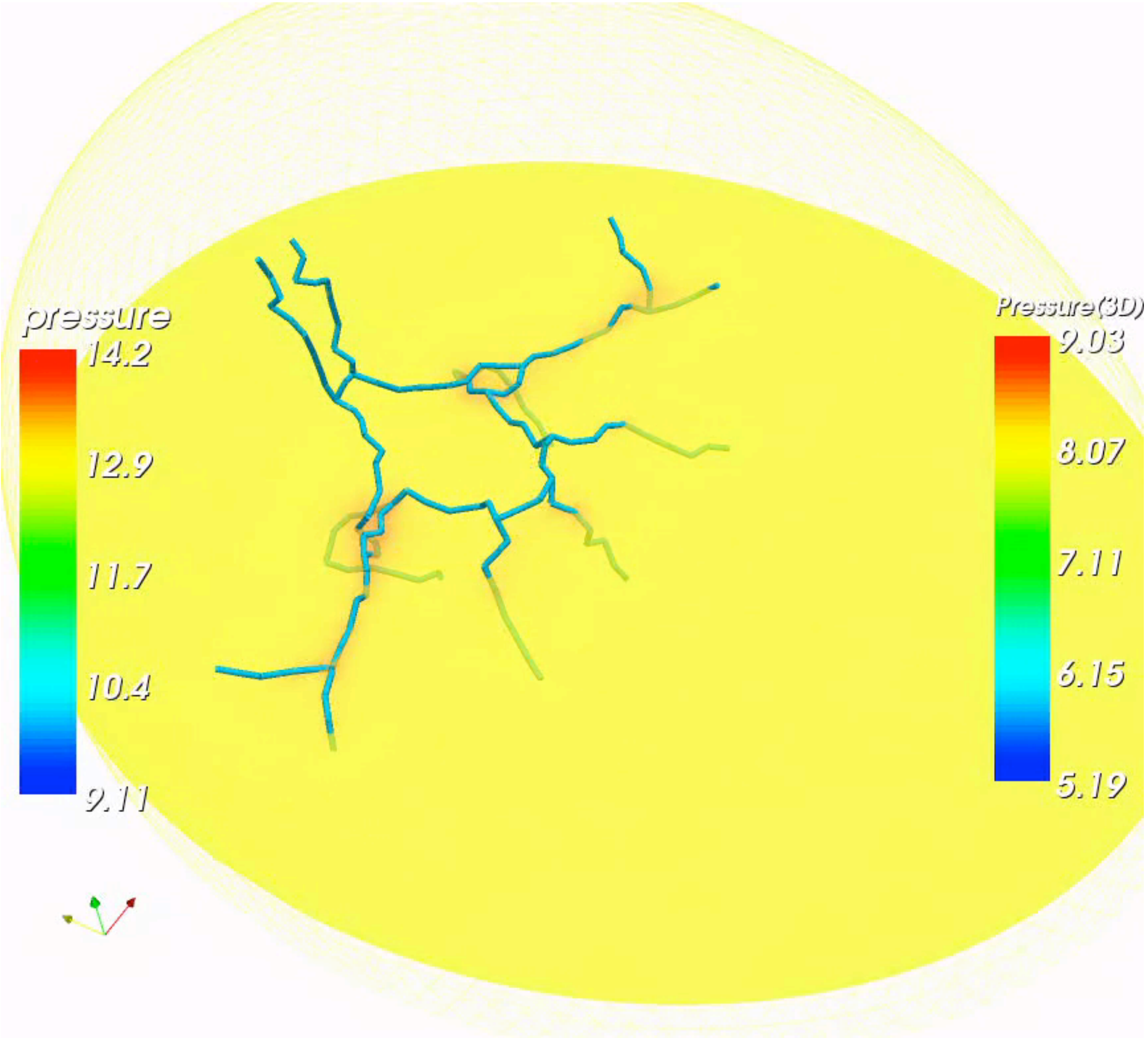

1D (vessels) and
3D (brain tissue)
blood pressures
with pulsatile input
blood flow rate and left
carotid artery occlusion

(Simulations by C.D'Angelo)

1D-3D Perfusion Model

A realistic time-dependent 1D-3D model:

$$\begin{cases} C_{\mathrm{t}} \dfrac{\partial}{\partial t} p_{\mathrm{t}} + \nabla \cdot (K_{\mathrm{t}} \nabla p_{\mathrm{t}}) + \alpha p_{\mathrm{t}} - \phi(p_{\mathrm{t}}, p_{\mathrm{v}}) \delta_{\Lambda} = 0 & t > 0, \ \mathbf{x} \in \Omega, \\ \dfrac{\partial}{\partial t} \begin{bmatrix} p_{\mathrm{v}} \\ q_{\mathrm{v}} \end{bmatrix} + \begin{bmatrix} 0 & \frac{1}{c} \\ \frac{1}{l} & 0 \end{bmatrix} \dfrac{\partial}{\partial s} \begin{bmatrix} p_{\mathrm{v}} \\ q_{\mathrm{v}} \end{bmatrix} + \begin{bmatrix} \frac{1}{c} \phi(p_{\mathrm{t}}, p_{\mathrm{v}}) \\ r q_{\mathrm{v}} \end{bmatrix} = \mathbf{0}, & t > 0, s \in \Lambda, \end{cases}$$

- $p_{\mathrm{t}} : \Omega \longrightarrow \mathbb{R}$ blood pressure in the tissue (3D)
- $p_{\mathrm{v}} : \Lambda \longrightarrow \mathbb{R}$ blood pressure in the vessel (1D)
- $q_{\mathrm{v}} : \Lambda \longrightarrow \mathbb{R}$ blood flow rate in the vessel (1D)
- $\phi : \Lambda \longrightarrow \mathbb{R}$ the exchange term

Flow model

$$\begin{cases} C_{\mathrm{t}} \dfrac{\partial}{\partial t} p_{\mathrm{t}} + \nabla \cdot (K_{\mathrm{t}} \nabla p_{\mathrm{t}}) + \alpha p_{\mathrm{t}} - \phi(p_{\mathrm{t}}, p_{\mathrm{v}}) \delta_{\Lambda} = 0 \quad t > 0, \ \mathbf{x} \in \Omega, \\ \dfrac{\partial}{\partial t} \begin{bmatrix} p_{\mathrm{v}} \\ q_{\mathrm{v}} \end{bmatrix} + \begin{bmatrix} 0 & \frac{1}{c} \\ \frac{1}{l} & 0 \end{bmatrix} \dfrac{\partial}{\partial s} \begin{bmatrix} p_{\mathrm{v}} \\ q_{\mathrm{v}} \end{bmatrix} + \begin{bmatrix} \frac{1}{c} \phi(p_{\mathrm{t}}, p_{\mathrm{v}}) \\ r q_{\mathrm{v}} \end{bmatrix} = \mathbf{0}, \qquad t > 0, s \in \Lambda, \end{cases}$$

- Venous transmission coefficients [range: 10^{-3} kPa^{-1} s^{-1}]
- Capillary compliance [10^{-3} kPa^{-1}]
- Tissue conductivity [0.05 mm^{2} kPa^{-1} s^{-1}]
- Vessel Windkessel parameters

1D-3D Perfusion Model

1D-3D mass transport and diffusion models:

$$\begin{cases} \dfrac{\partial}{\partial t}u_{\mathrm{t}} - D_{\mathrm{t}}\Delta u_{\mathrm{t}} + \mathbf{v}\cdot\nabla u_{\mathrm{t}} - \theta(u_{\mathrm{t}}, u_{\mathrm{v}})\delta_{\Lambda} = f, \ t > 0, \ \mathbf{x} \in \Omega, \\ A_0\dfrac{\partial}{\partial t}u_{\mathrm{v}} - A_0 D_{\mathrm{v}}\dfrac{\partial^2 u_{\mathrm{v}}}{\partial s^2} + q_{\mathrm{v}}\dfrac{\partial}{\partial s}u_{\mathrm{v}} = 0, \qquad t > 0, s \in \Lambda, \end{cases}$$

$u_{\mathrm{t}} : \Omega \to \mathbb{R}$ mass concentration in the tissue (3D)

$u_{\mathrm{v}} : \Lambda \to \mathbb{R}$ mass concentration in the vessel (1D)

$\theta = \frac{1}{\epsilon}(u_{\mathrm{v}} - \bar{u}_{\mathrm{t}})$ is a penalization term.

- Same form as ϕ
- Enforces $u_{\mathrm{v}} = \bar{u}_{\mathrm{t}}$

Computing -
Complexity

FSI algorithms

The Coupled FS system in compact form

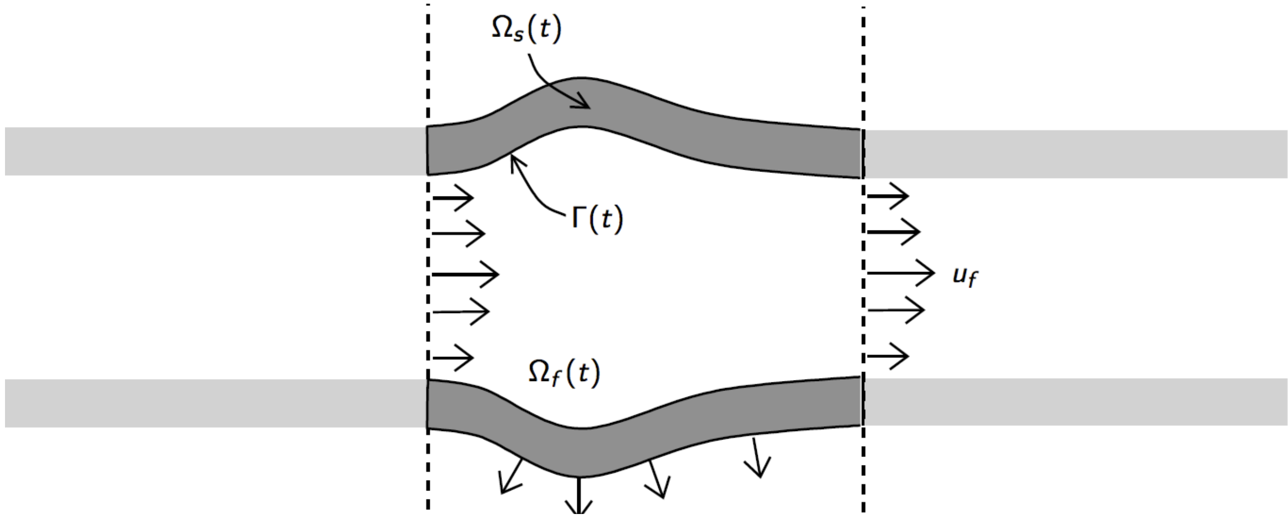

- ***FS system***
  With variables (u_f, d_f, d_s) *for the fluid solution and displacements of the fluid and structure domain respectively, the fluid-structure interaction problem is*

$$\begin{aligned} F(u_f, d_s, d_f) &= 0, && \text{fluid subproblem} \\ S(u_f, d_s) &= 0, && \text{structure subproblem} \\ G(d_s, d_f) &= 0 && \text{geometry subproblem.} \end{aligned}$$

Fluid structure Interaction (FSI) - Not only blood flow

- ***Aerodynamics***

  Aircrafts, Flying Bodies

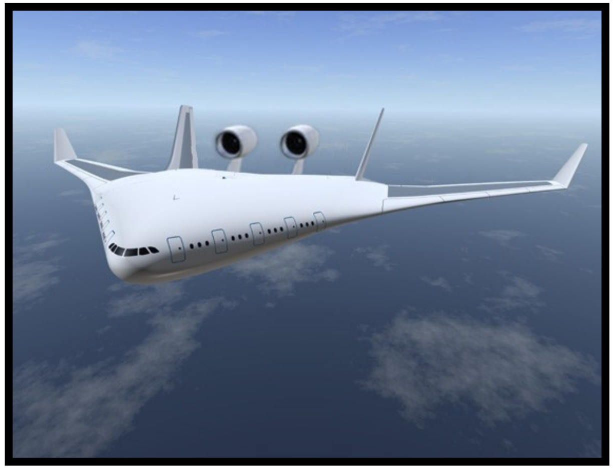

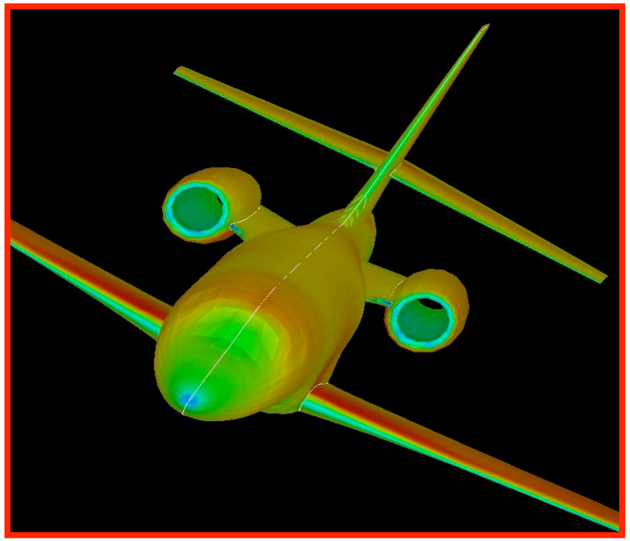

- ***Wing Multihulls***

  Wind-sail interaction

Fluid structure Interaction (FSI)

Rowing and sea-keeping

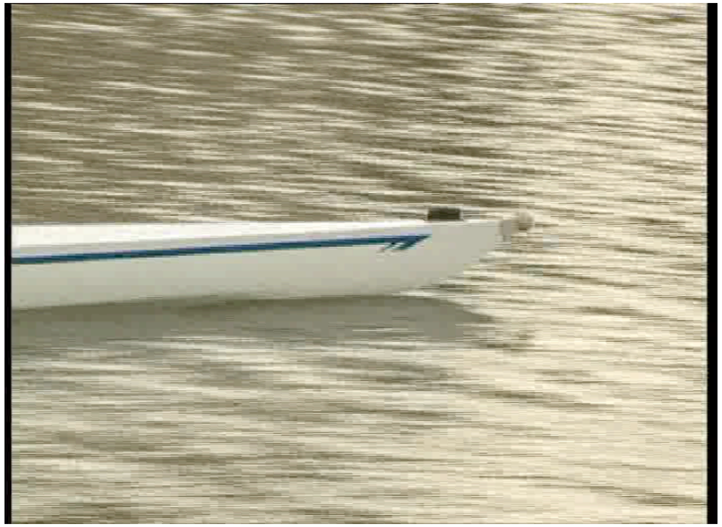

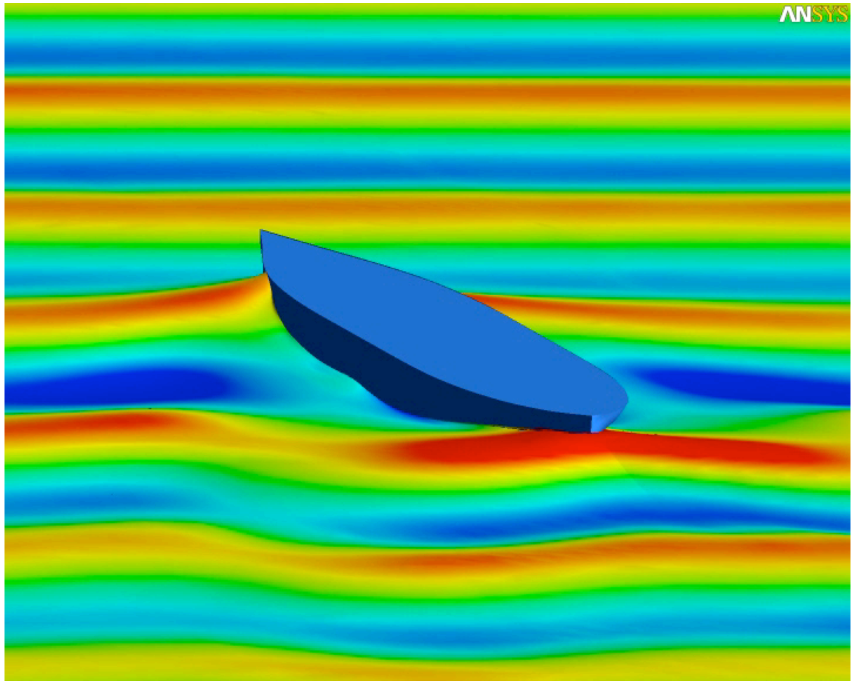

Swinsuits optimization (A.Veneziani,N.Parolini)

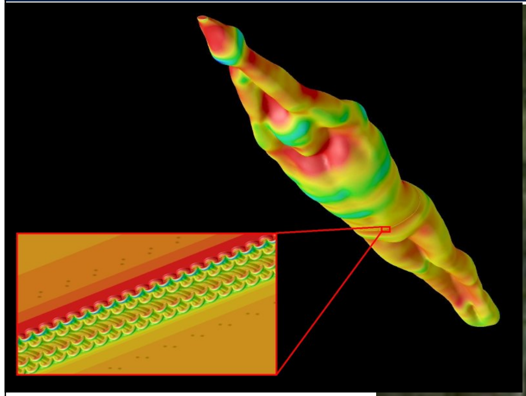

POWERSKIN Xtreme

Wind/sails interaction

(N.Parolini, D.Detomi)

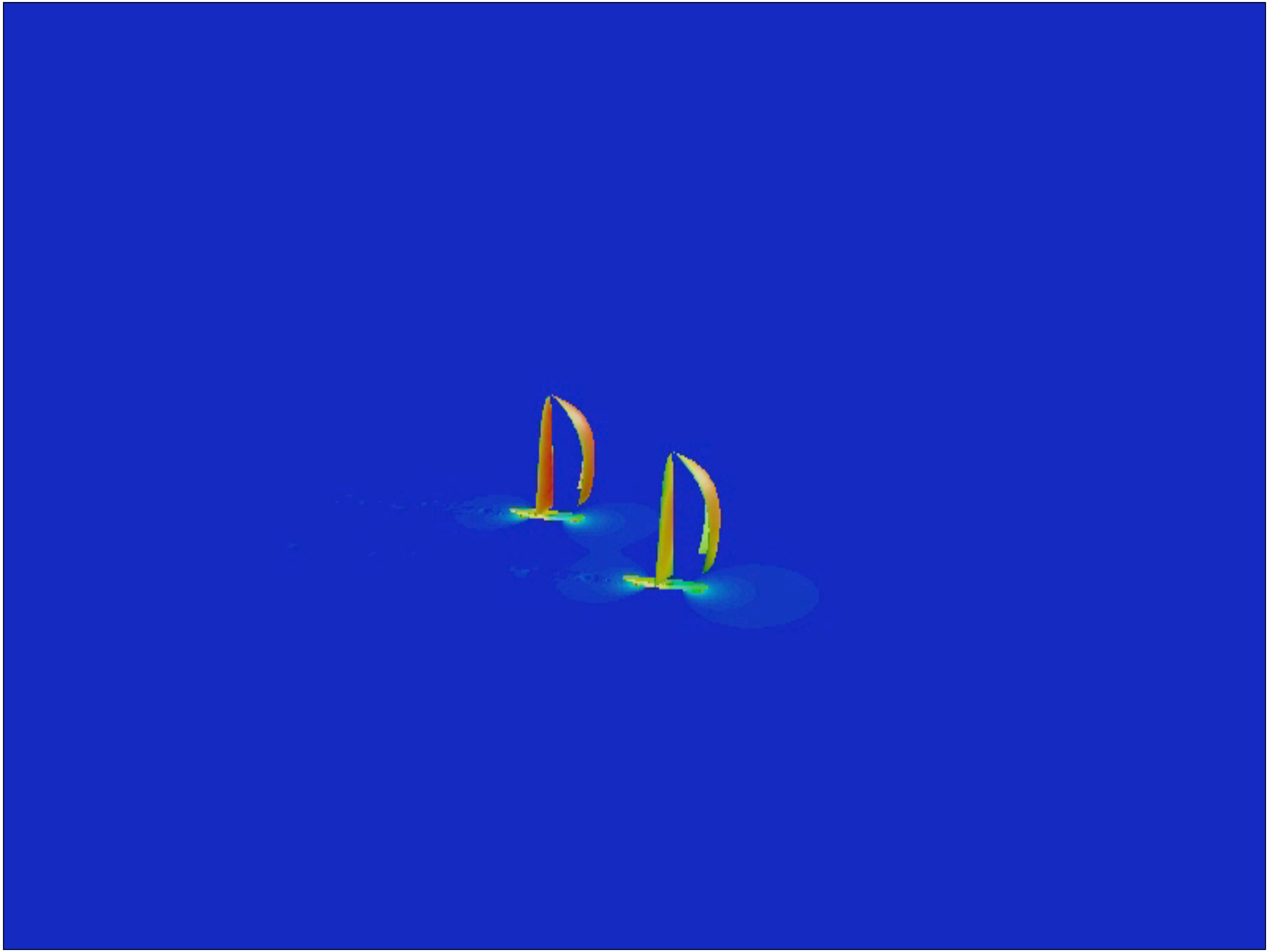

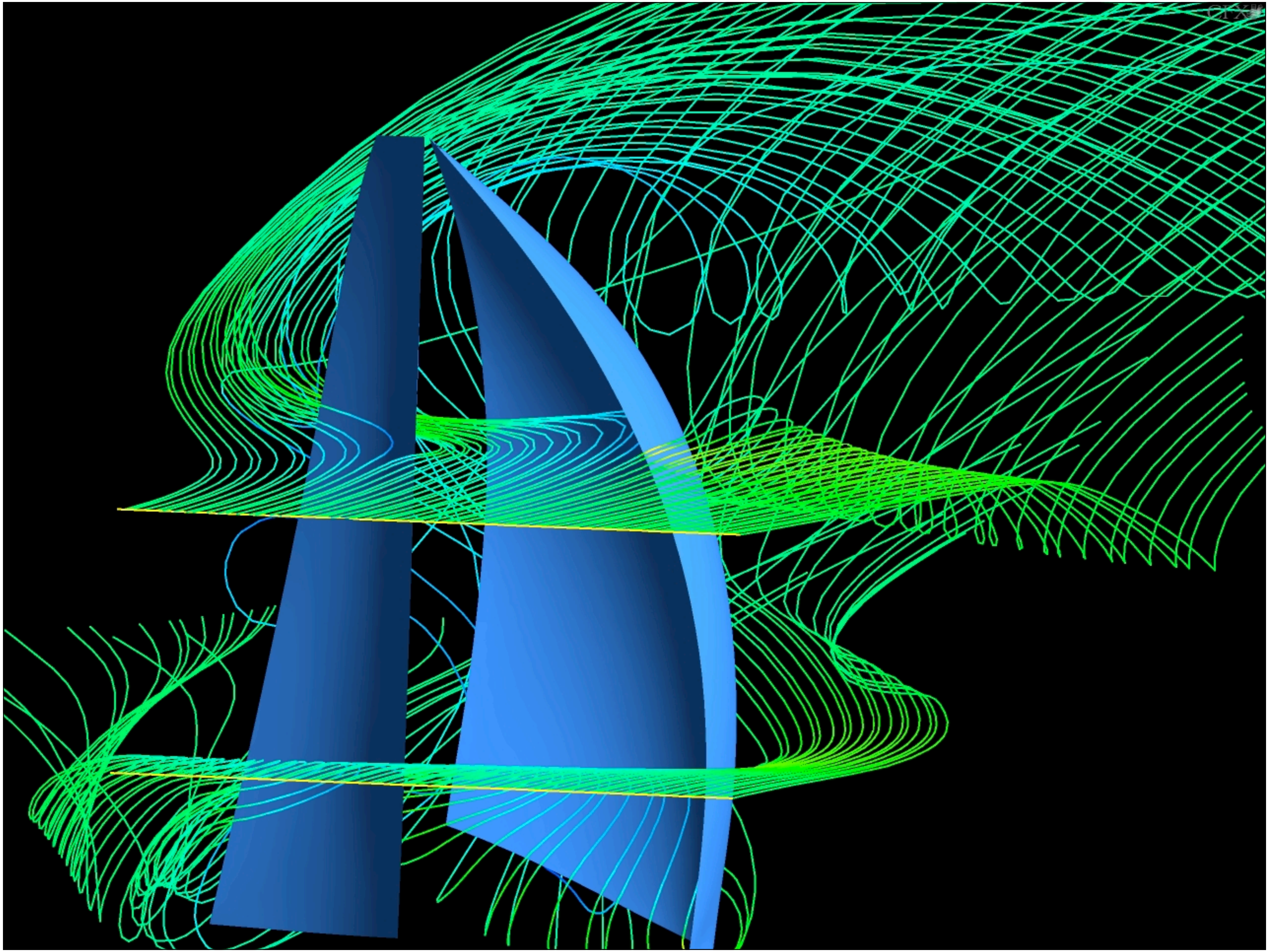

FSI - Numerical Algorithms

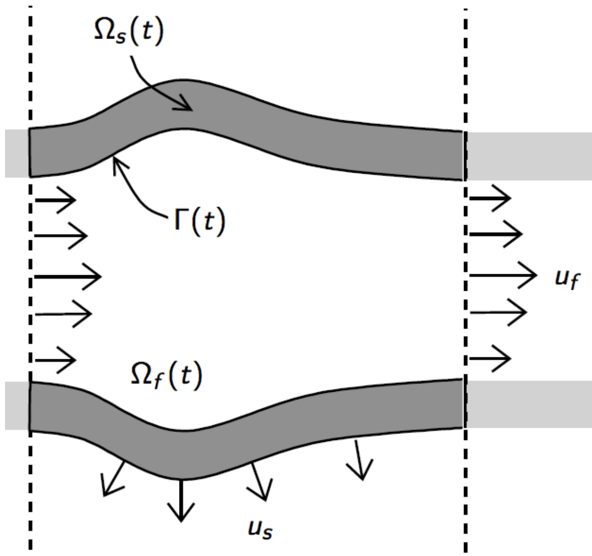

$$F(u_f, d_s, d_f) = 0,$$
$$S(u_f, d_s) = 0,$$
$$G(d_s, d_f) = 0$$

Solution approach: FEM in space, FD in time, then:

Segregated / Monolithic / Hybrid

- Newton linearization
- Krylov iterative methods
- Domain Decomposition preconditioners

based on blockwise parallel Schwarz preconditioners

(P.Crosetto, S.Deparis, G.Fourestey, A.Q,
Parallel Algorithms for Fluid Structure Interaction Problems in Haemodynamics, SIAM J. Sci. Comp., 2011)

Reduction to the interface problem

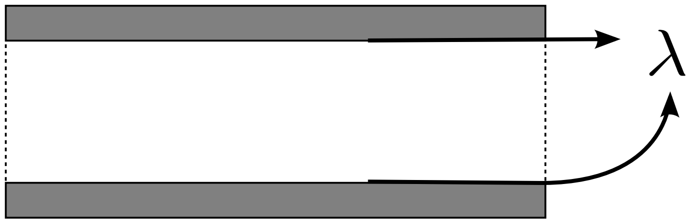

Goal: eliminate fluid, structure and geometric variables

Let us define The Steklov-Poincaré operators for the fluid and structure subdomains as

$$\begin{array}{llll} S_f : & H^{1/2}(\Gamma)^3 & \rightarrow & H^{-1/2}(\Gamma)^3 \\ & \lambda = \mathbf{d}_{s\Gamma} & \mapsto & \boldsymbol{\sigma}_f^o|_\Gamma \\ S_s : & H^{1/2}(\Gamma)^3 & \rightarrow & H^{-1/2}(\Gamma)^3 \\ & \lambda = \mathbf{d}_{s\Gamma} & \mapsto & \boldsymbol{\sigma}_s|_\Gamma \end{array} \qquad (17)$$

that map the trace space of displacements on the interface Γ to the dual space of the normal stresses exerted on Γ.

Applications

Understanding Physiology

Subdomain partition for lumen and wall

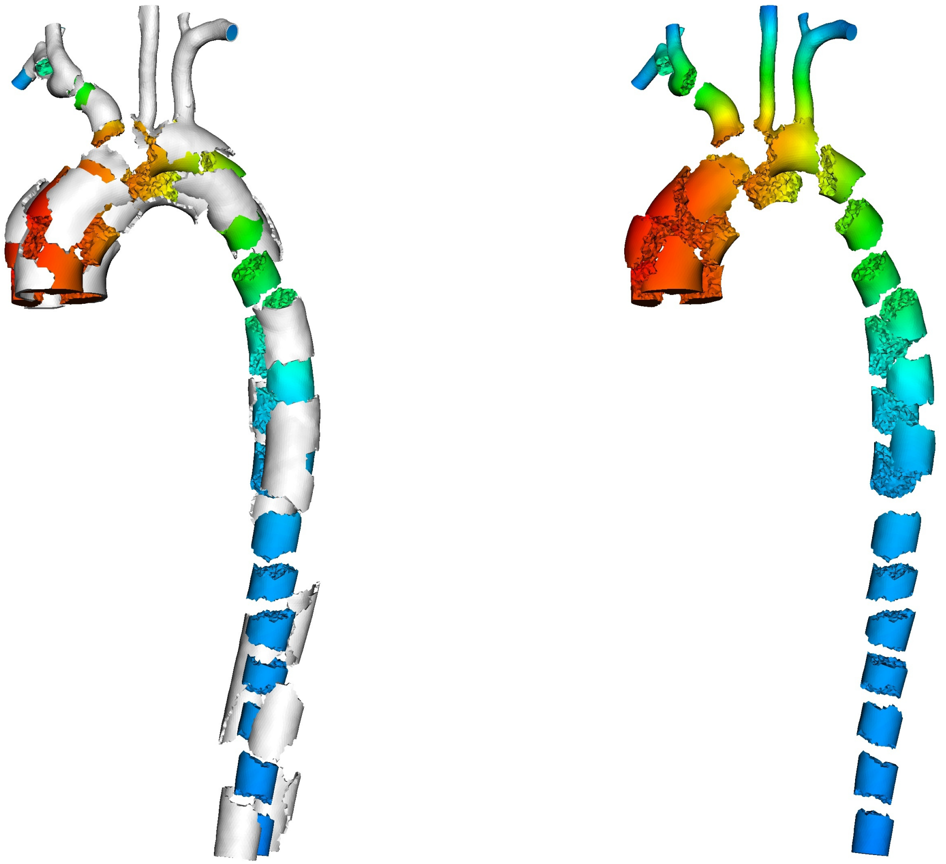

FIGURE: The fluid and the solid meshes are partitioned in 2x32 subdomains. 380′690 tetrahedra and 324′000 dofs

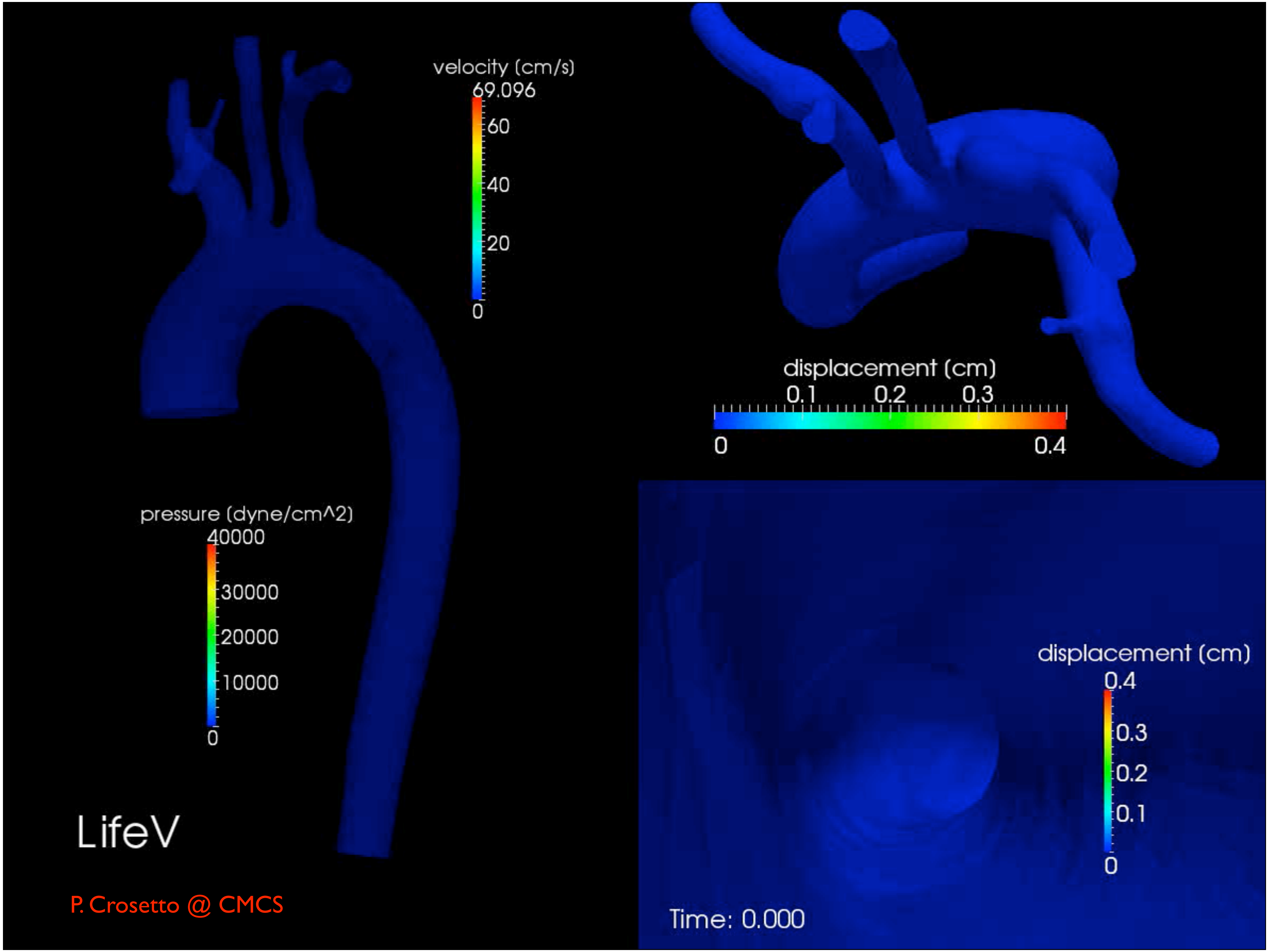
velocity (cm/s)
69.096
60
40
20
0
displacement (cm)
0.1
0.2
0.3
0
0.4
pressure (dyne/cm^2)
40000
30000
20000
10000
0
displacement (cm)
0.4
0.3
0.2
0.1
0
LifeV
P. Crosetto @ CMCS
Time: 0.000

FSI in the aortic arch: WSS comparisons

Compliant versus rigid walls: WSS pattern at systole

The rigid walls simulation (middle) shows important differences in WSS

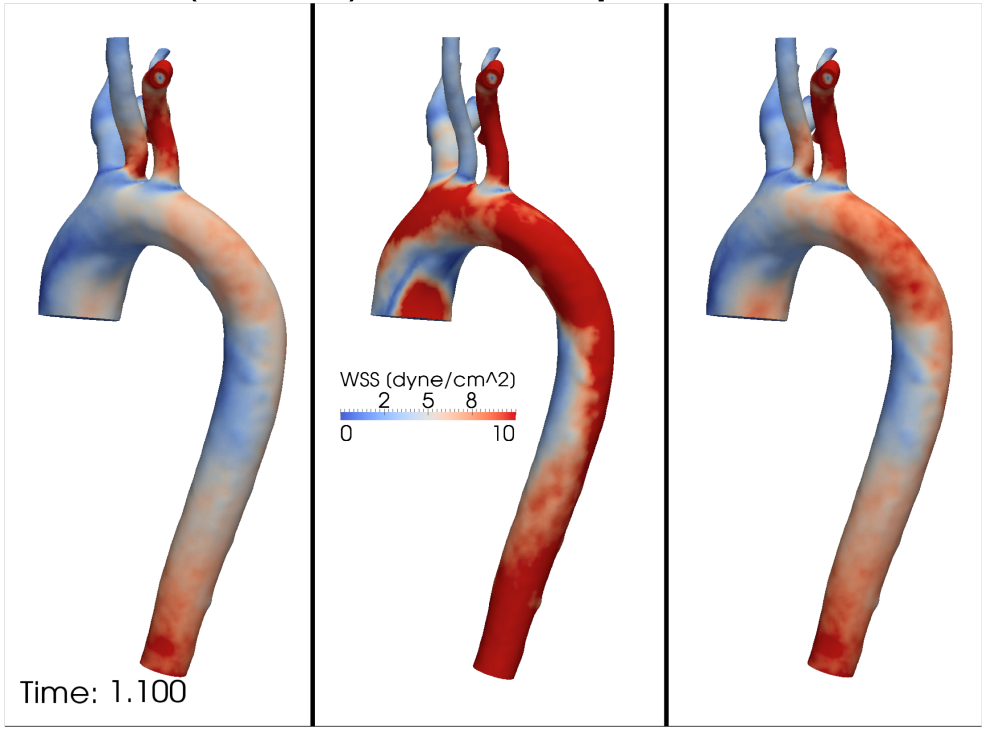

Compliant, inlet flux Rigid Compliant, inlet pressure

Patient-specific geometry and boundary conditions. Simulation run for 3 heartbeats, timings: about 30s per timestep, 6.6h per heartbeat (800 timesteps), using 128 processors on Cray XT6 cluster HECToR (www.hector.ac.uk)

(Crosetto, Reymond, Deparis, Kontaxakis, Stergiopulos, AQ, submitted, 2011)

FSI in the aortic arch: WSS comparisons

Compliant versus rigid walls:
history of space averages at different locations

WSS mainly overestimated by the rigid wall simulation, differences in magnitude and waveform

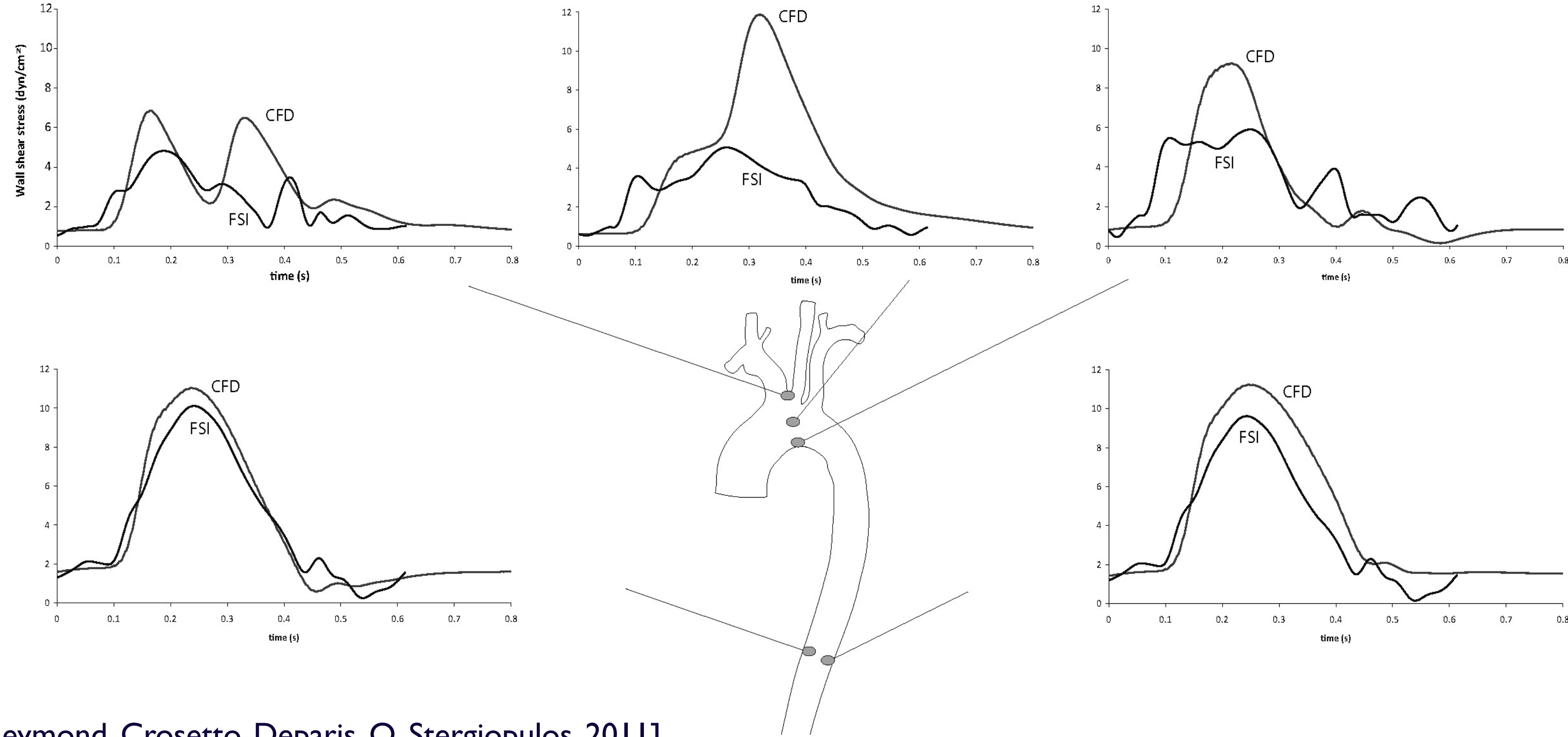

[Reymond, Crosetto, Deparis, Q, Stergiopulos, 2011]

Flow in the iliac artery

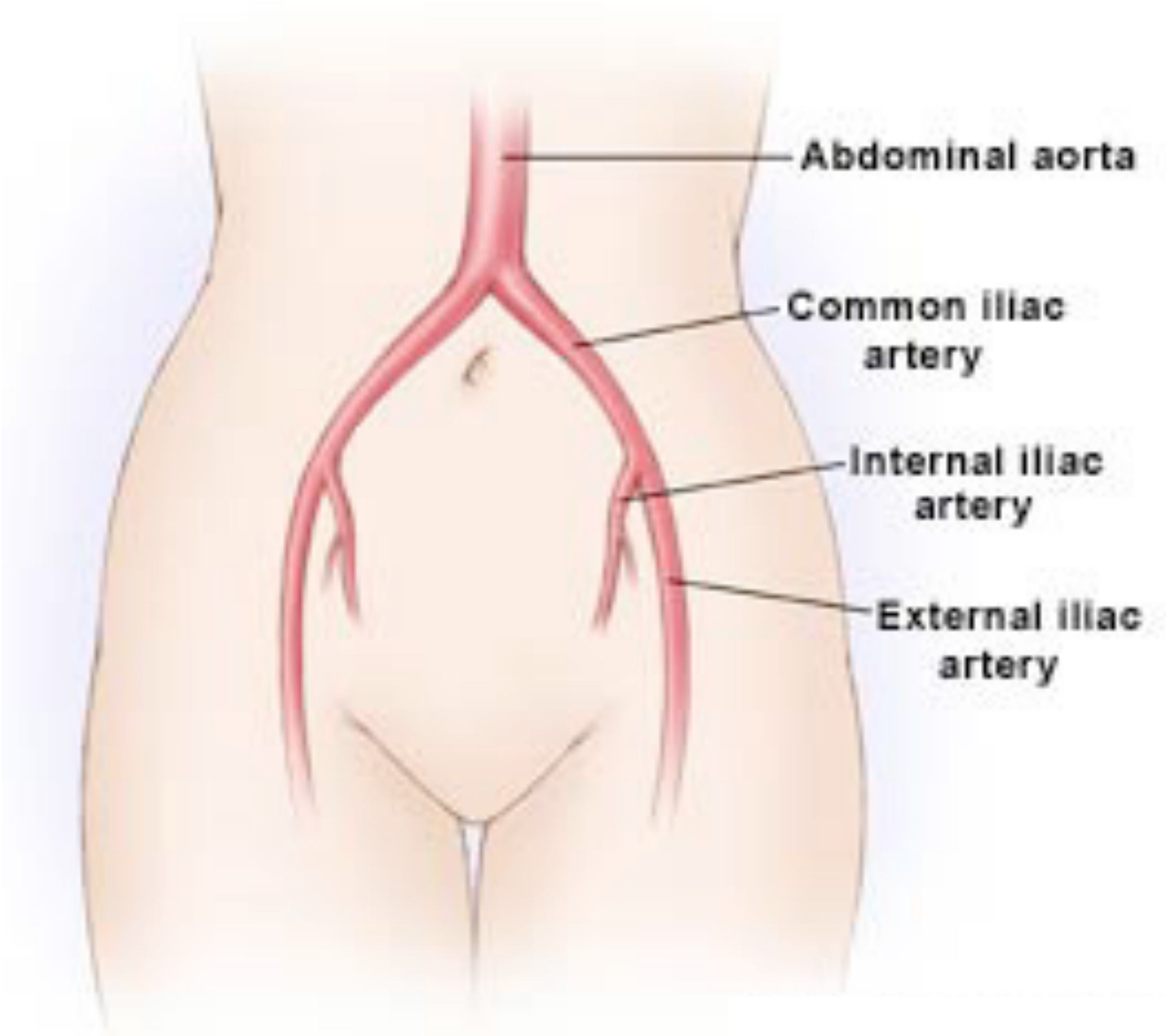

Flow in an iliac artery

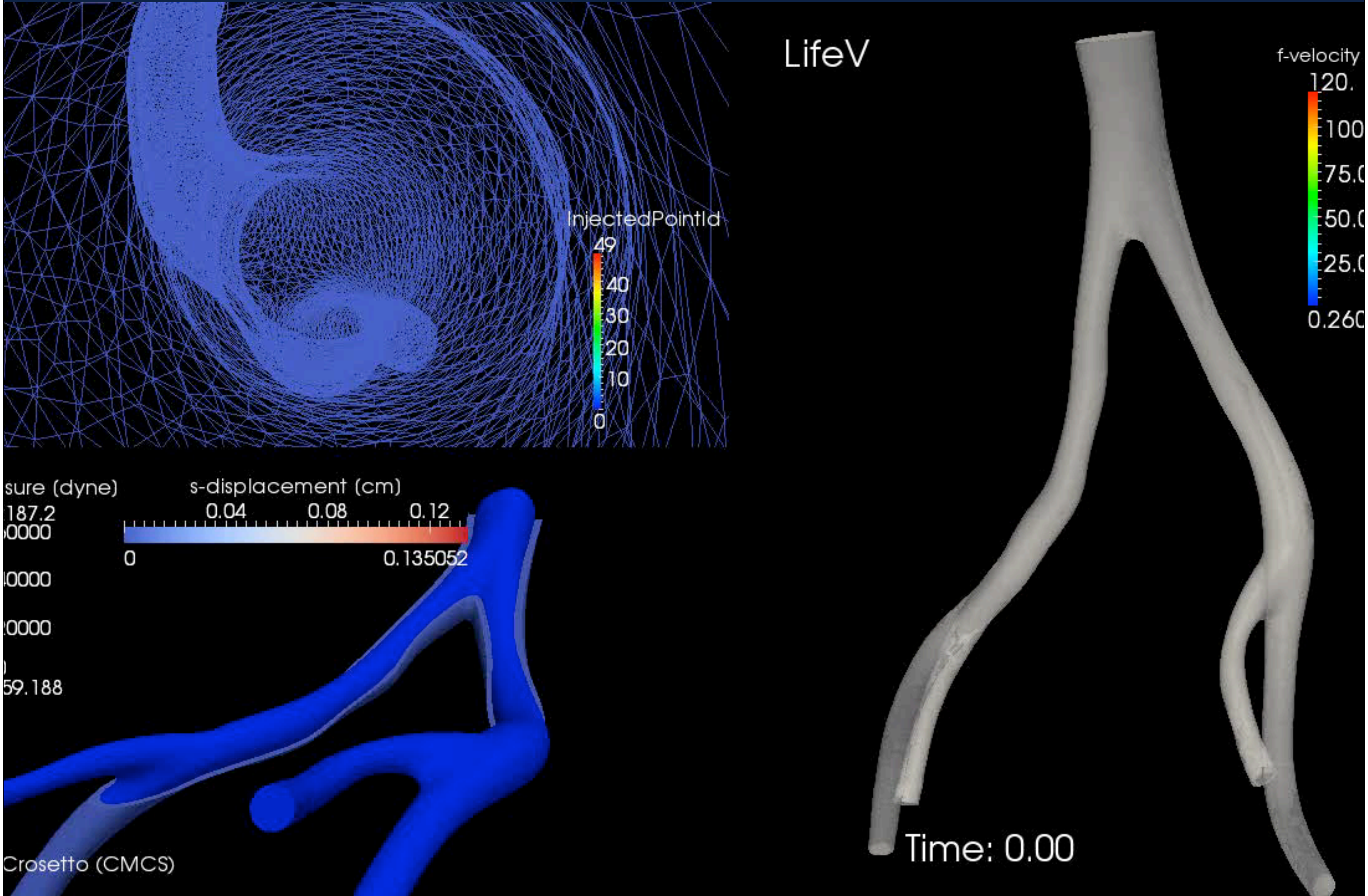

Applications

Surgical Planning

Bypass graft in abdominal artery

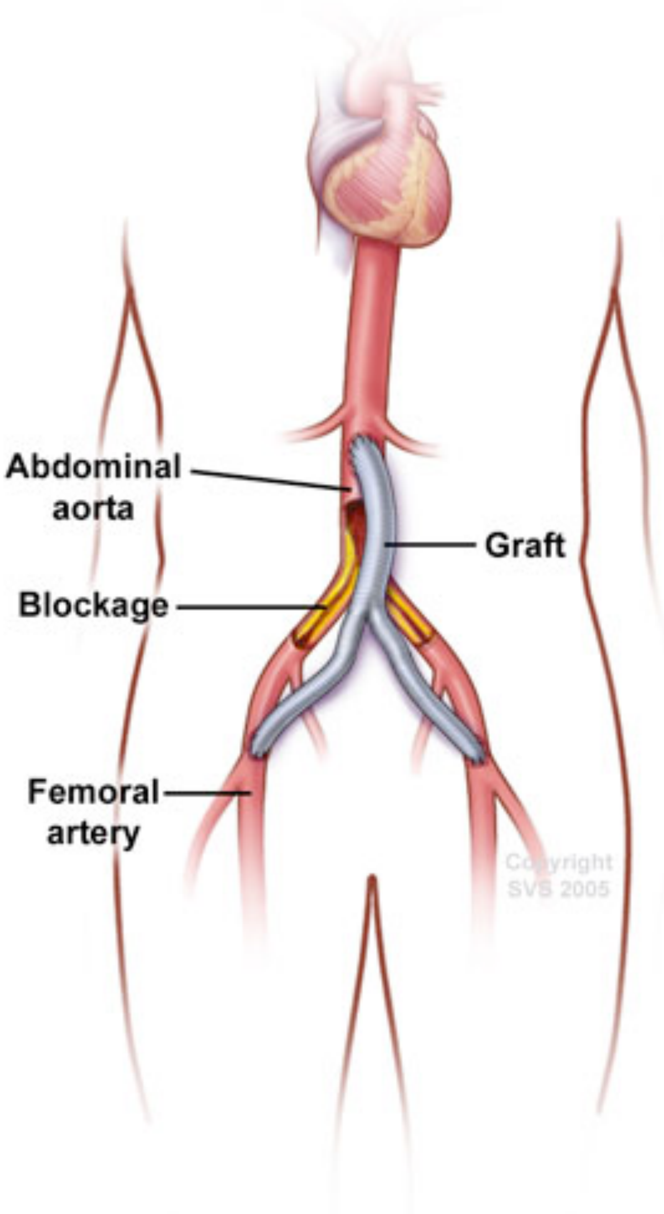

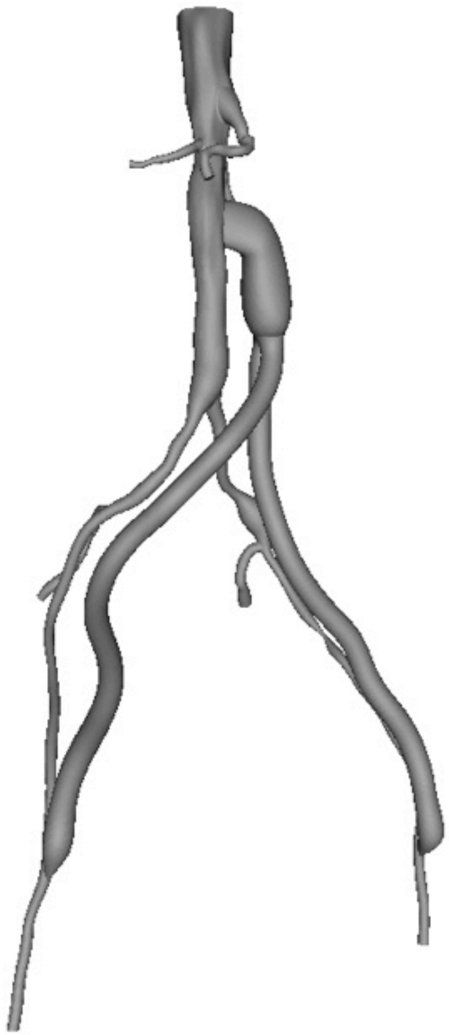

WSS and streamlines at systole

Recirculation zone at the bypass anastomosis (left) produces modification in the WSS pattern (right)

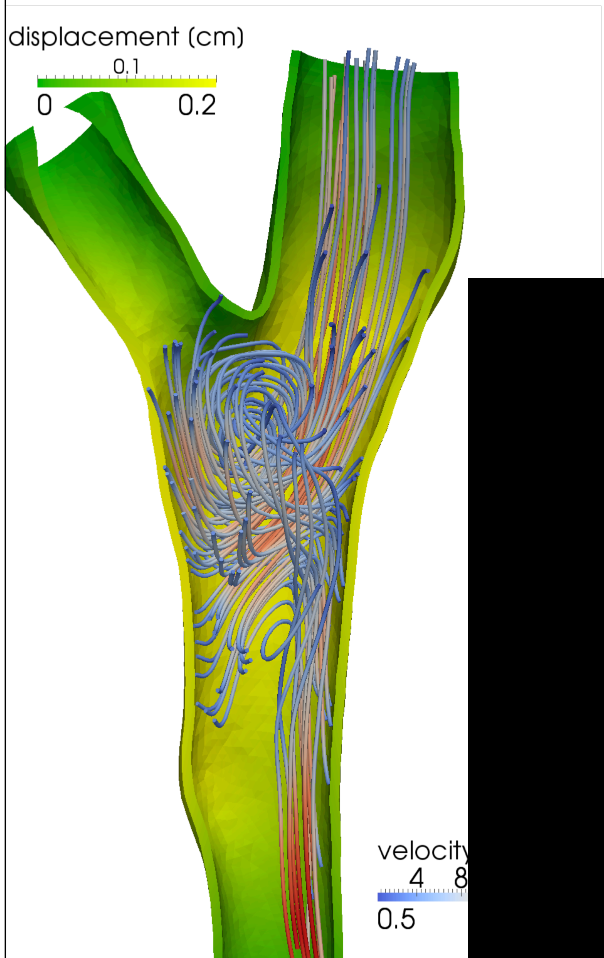

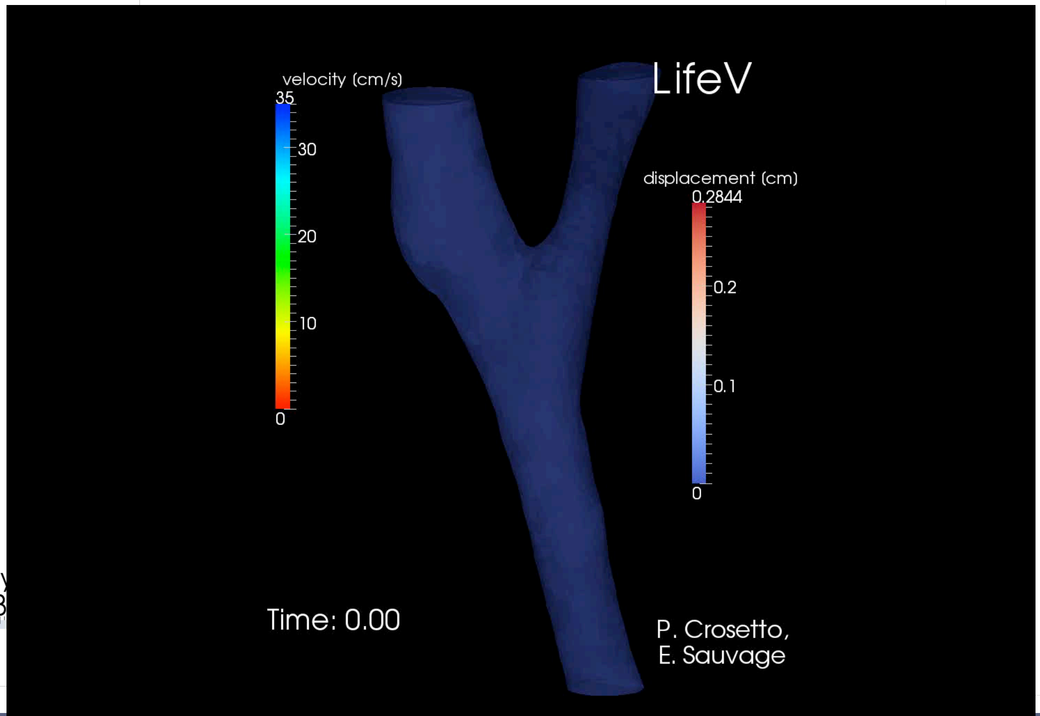

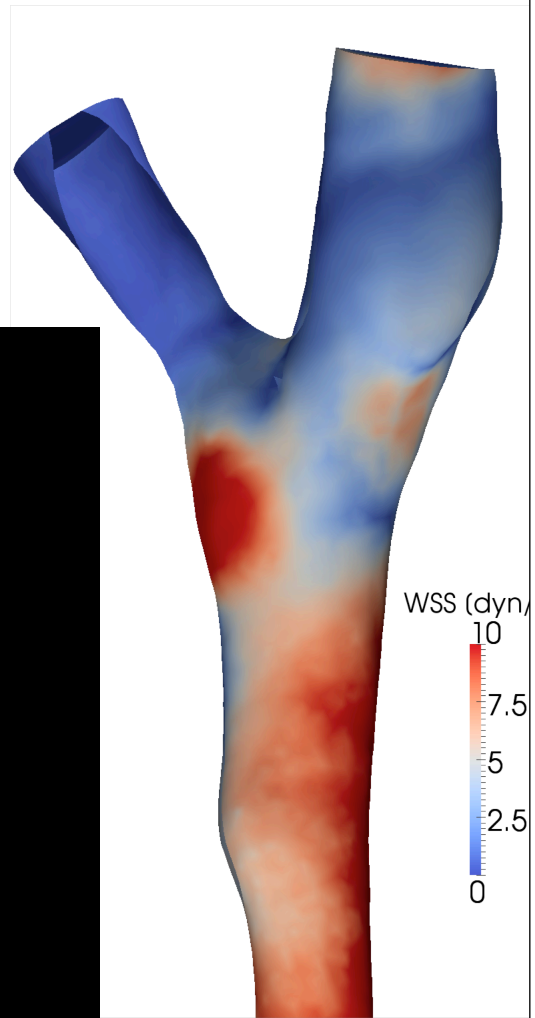

Flow in Cerebral Aneurysms

Cerebral aneurysms: deformations of cerebral arteries, mostly placed on vessels belonging to or connected to the Circle of Willis.

EPIDEMIOLOGICAL STATISTICS

- Incidence rate of cerebral aneurysms:

  1/20 people

- Incidence rate of ruptured cerebral aneurysms per year:

  1/10000 people per year

- Mortality due to a ruptured aneurysm:

  > 50%:

Out of 9 patients with a ruptured aneurysm:

- 3 are expected to die before arriving at the hospital
- 2 to die after having arrived at the hospital
- 2 to survive with permanent cerebral damages
- 2 to survive without permanent cerebral damages

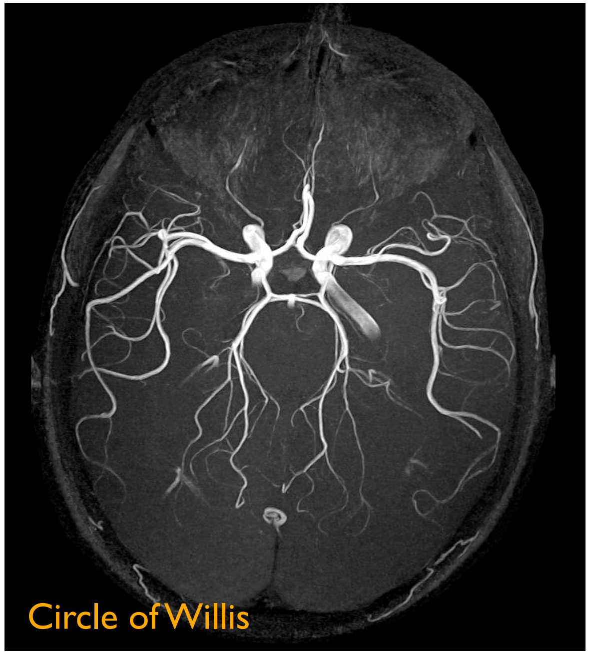

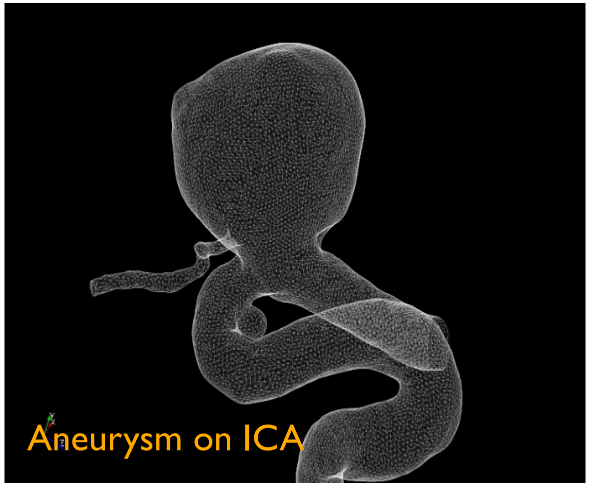

Flow in a cerebral aneurysm during a full cardiac pulse

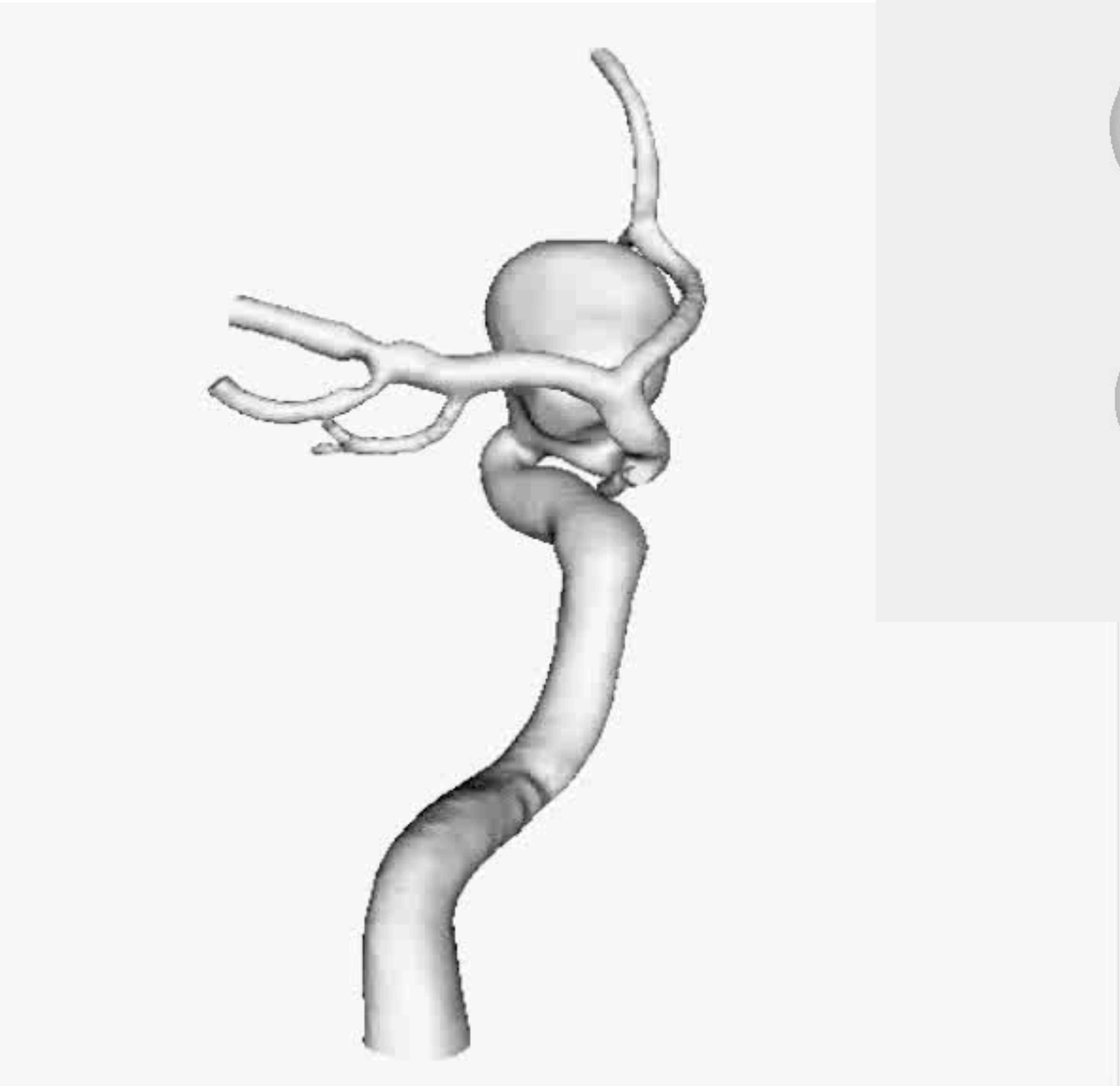

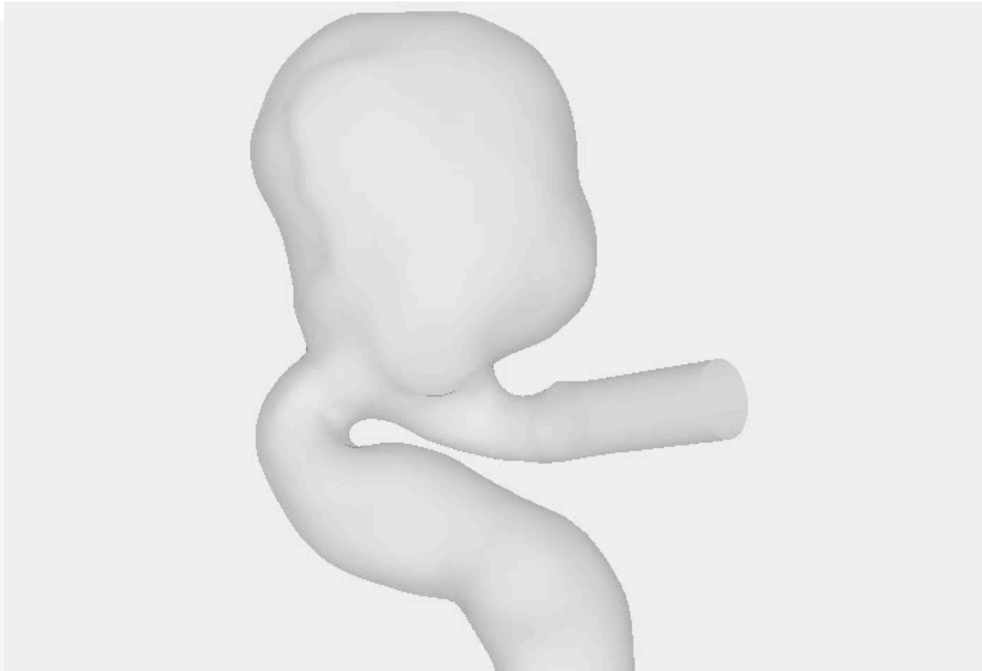

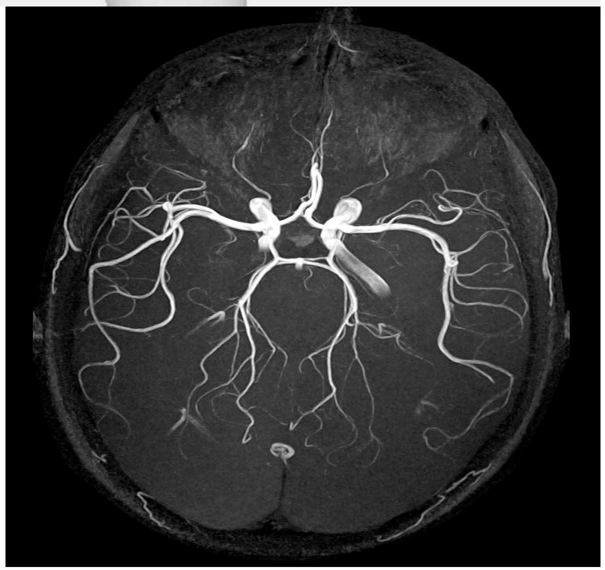

Simulation carried out by T. Passerini

Pressure, velocity and wall displacement

$dofs = 100'000$, $dt = 10^{-3}$, $T = .9$, $cpus = 32$,
P1P1-IP, FSI: Segr. inexact Newton,

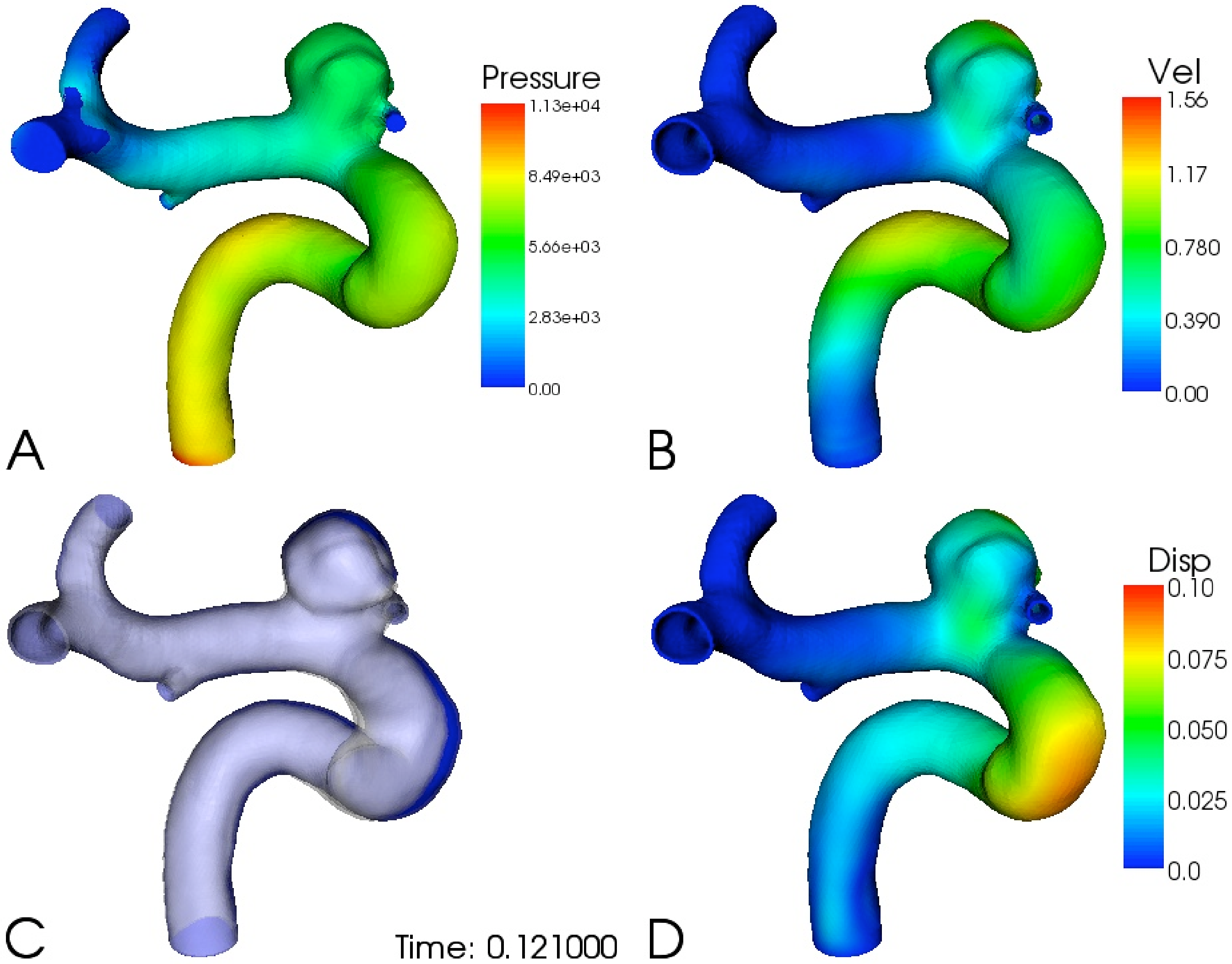

WSS - Wall Shear Stress

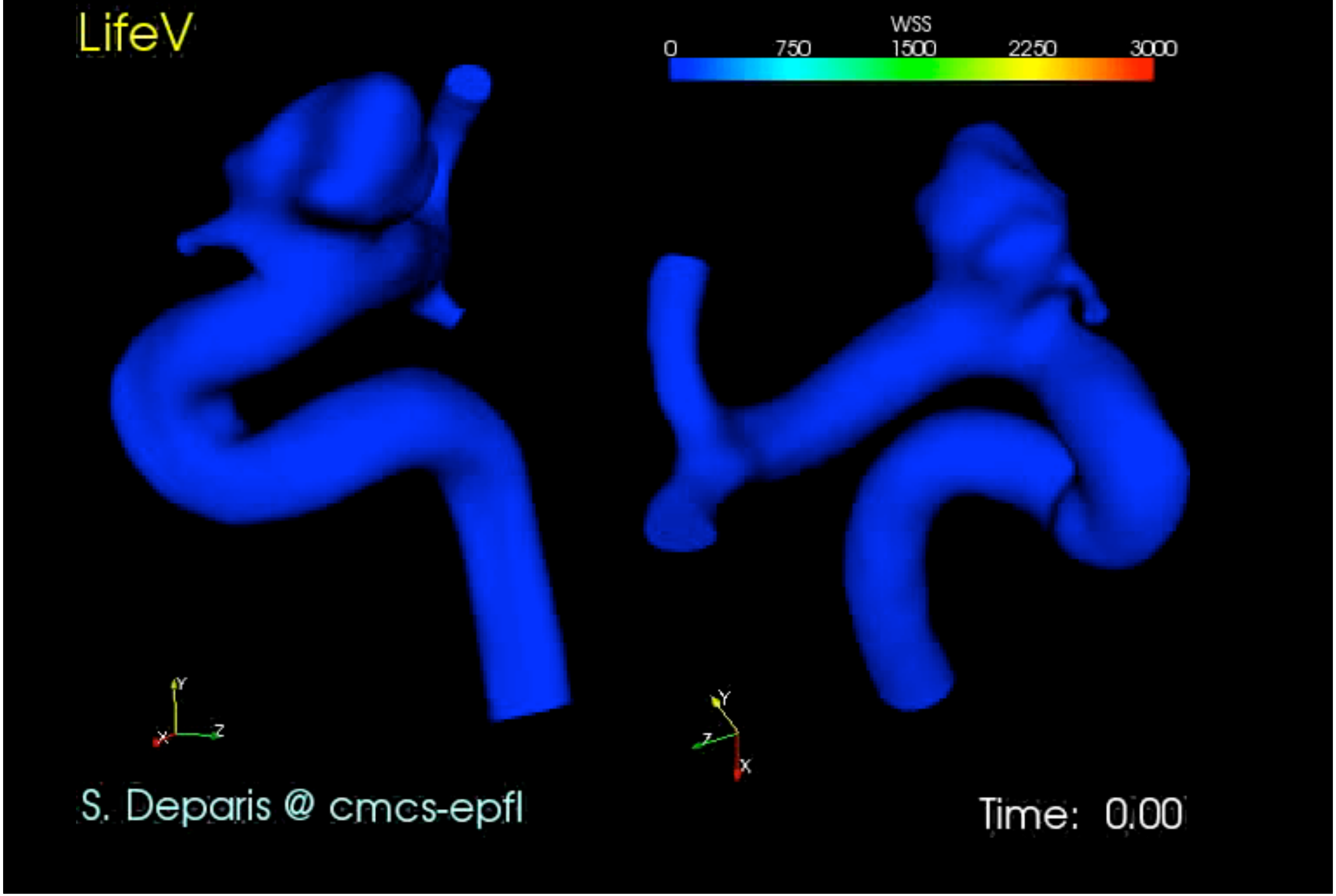

Applications

Prosthetic Devices

Cannula of a Ventricular Assisted Device (VAD)

VAD connection to an Aorta (6 lt/min blood supply)

WSS and streamlines (steady state simulation)

Recirculation and secondary flows (left/lower right) velocity magnitude (upper right)

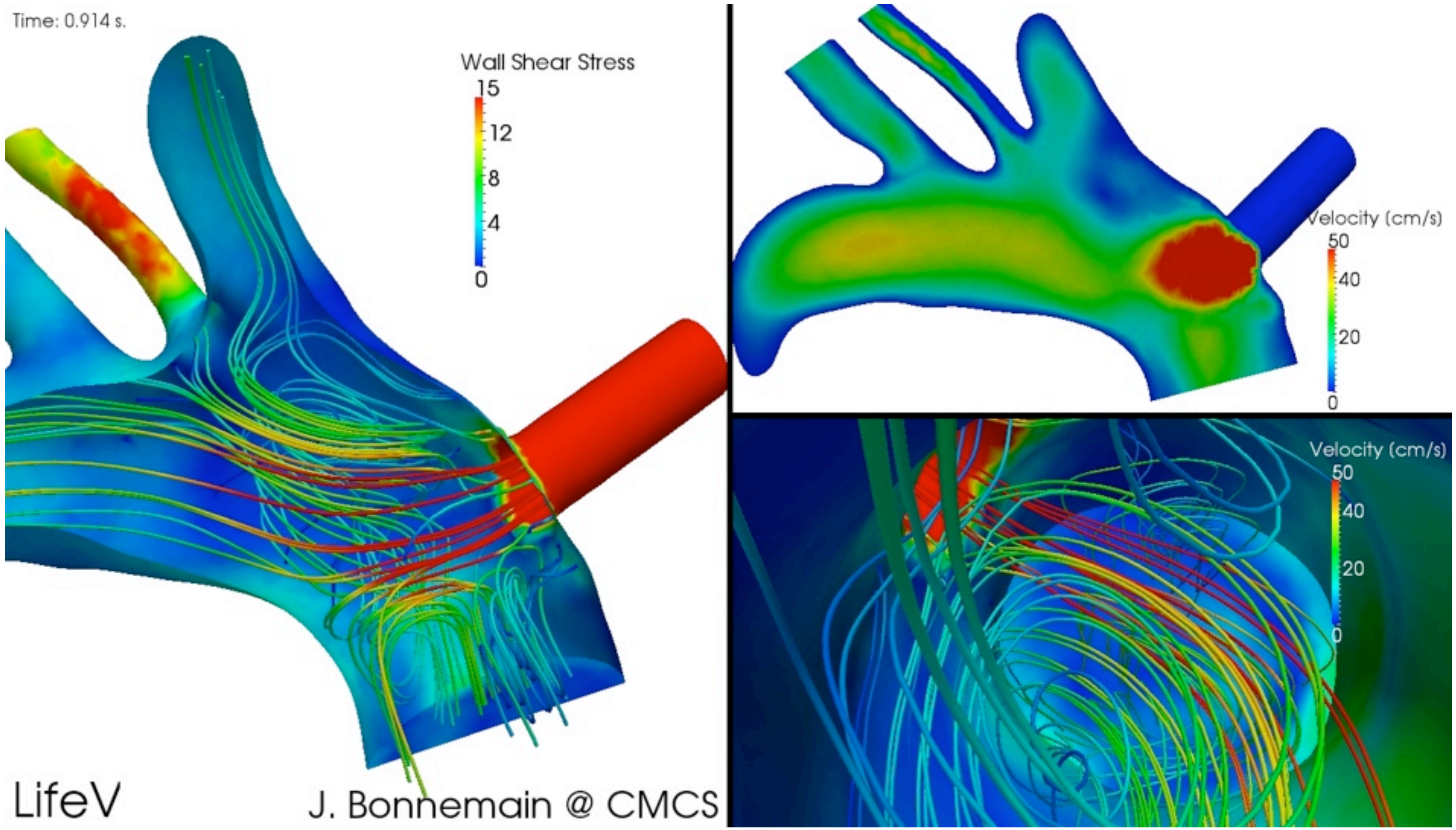

Cannula of a Ventricular Assisted Device to Aorta

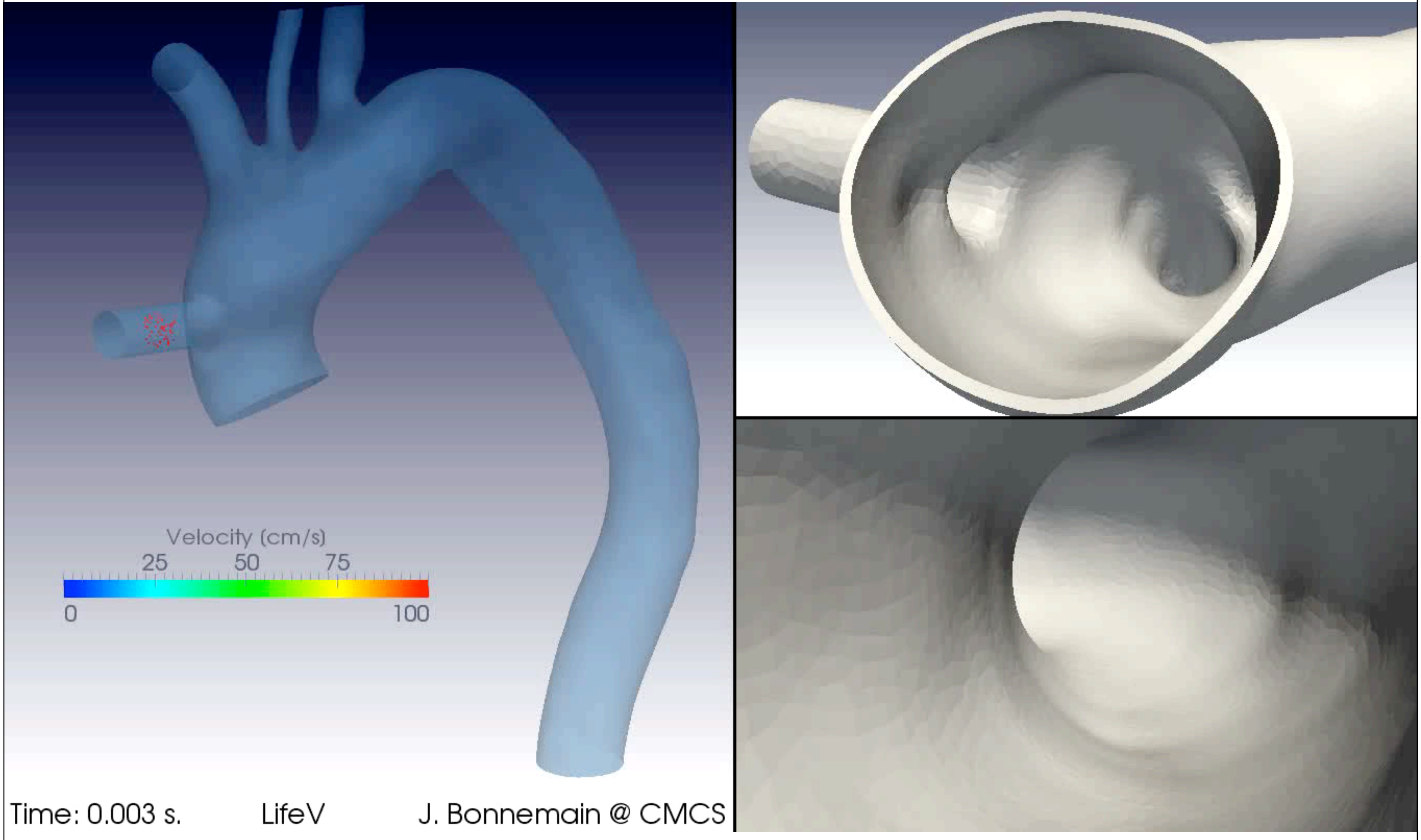

Drug release from Stents

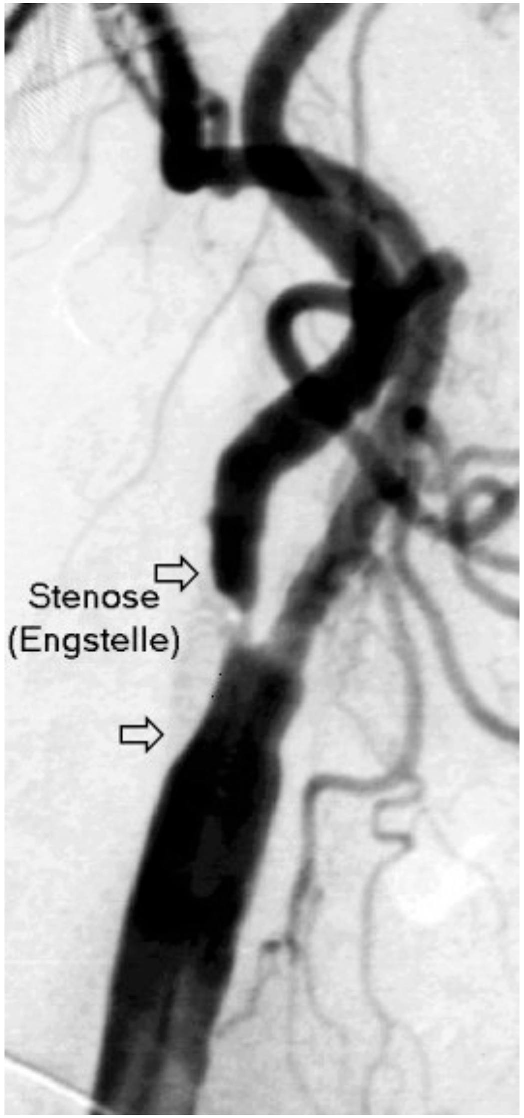

Angiography after stent placement

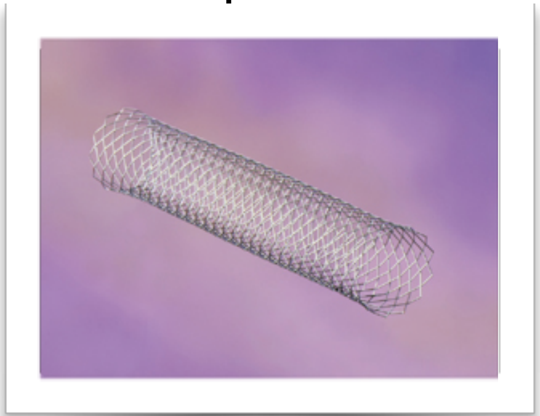

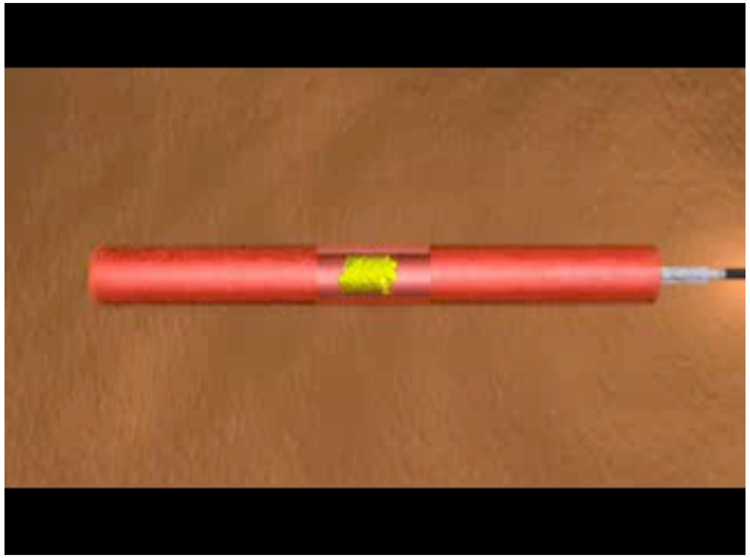

Drug release from Stents

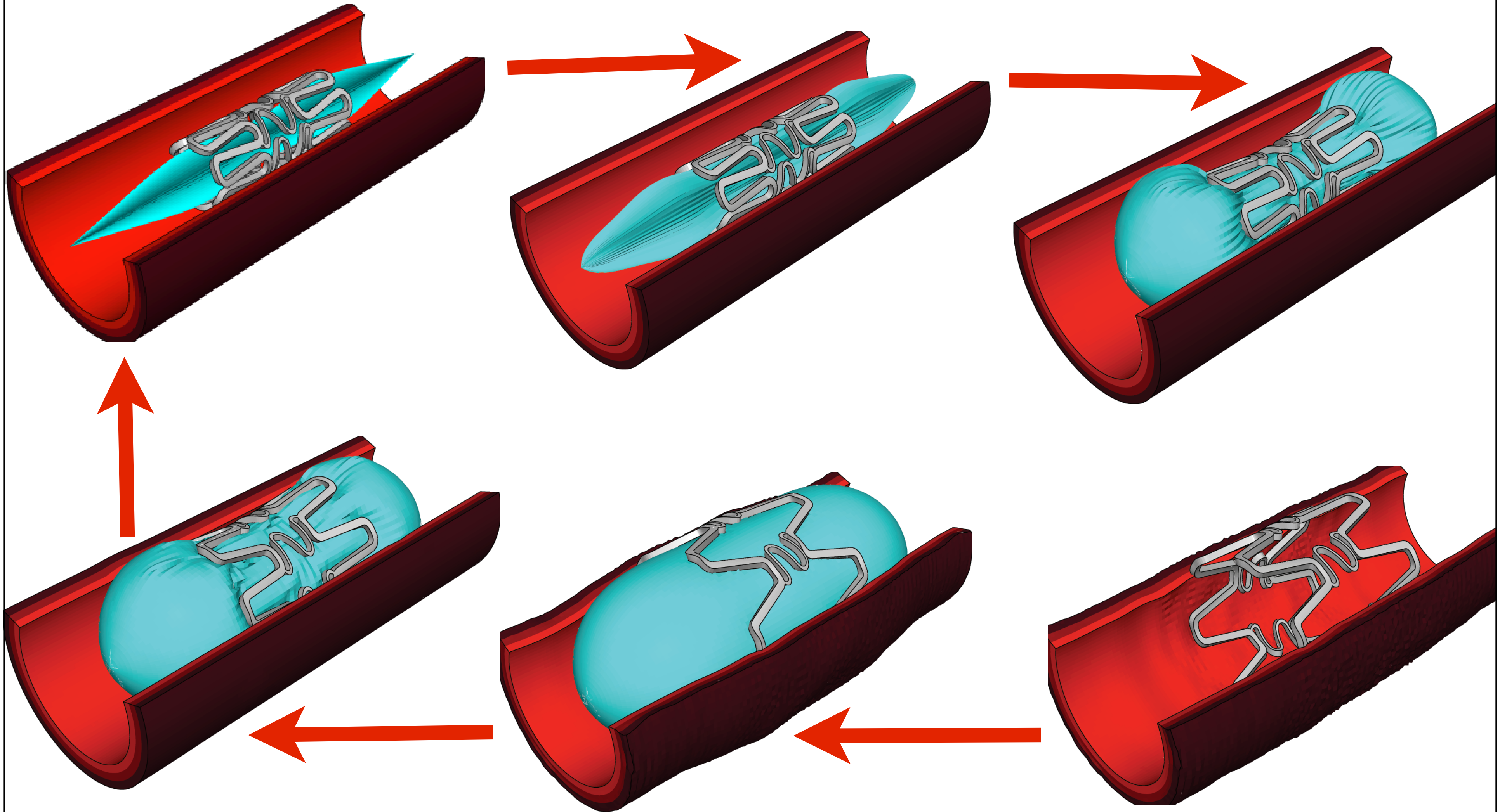

Stent deployment (Courtesy of LABS-Polimi)

A Multi-Domain/Multi-Phase Problem

Macroscale, mm (in the arterial wall)

$$\frac{\partial c}{\partial t} = D\Delta c + \mathbf{u}\nabla c$$

Macroscale, μm (in the coating matrix)

$$\frac{\partial C_L}{\partial t} = \underbrace{\frac{1}{r^2}\frac{\partial}{\partial r}\left(D \cdot r^2 \cdot \frac{\partial C_L}{\partial r}\right)}_{\text{Diffusion}} + \underbrace{C_{Se} \cdot K_{Lero}}_{\text{Erosion}} - \underbrace{\frac{\partial C_{Se}}{\partial t}(1 - K_{Lero} \cdot t)}_{\text{Dissolution}}$$

LIQUID PHASE

$$\frac{\partial C_S}{\partial t} = -\frac{\partial C_{Se}}{\partial t}(1 - K_{Lero} \cdot t) - C_{Se} \cdot K_{Lero}$$

VIRTUAL SOLID PHASE (free interface)

$$\frac{\partial C_{Se}}{\partial t} = -K_{dis}(\epsilon C_{sat} - C_L)$$

EFFECTIVE SOLID PHASE (dynamics of polymer concentration)

K_{dis}, K_{Lero}, D

Depend on polymer characteristics (porosity, tortuosity,...)
Determined by stochastic models

Flow Field Around a Stent: Numerical Simulation

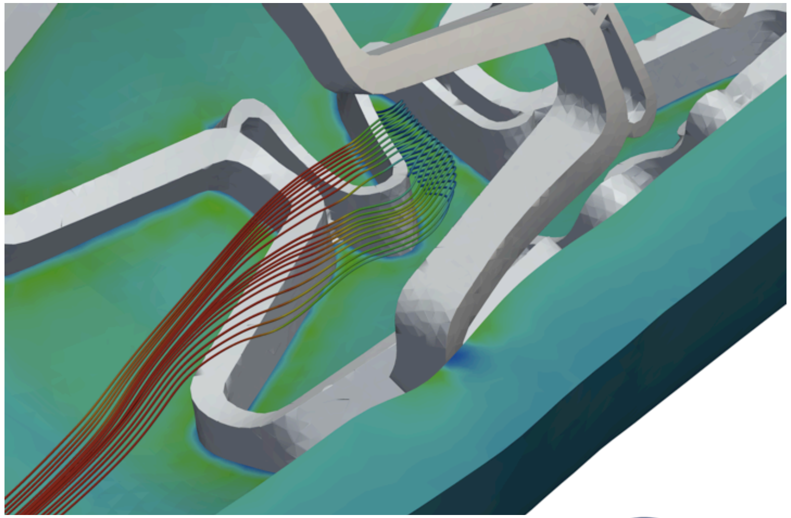

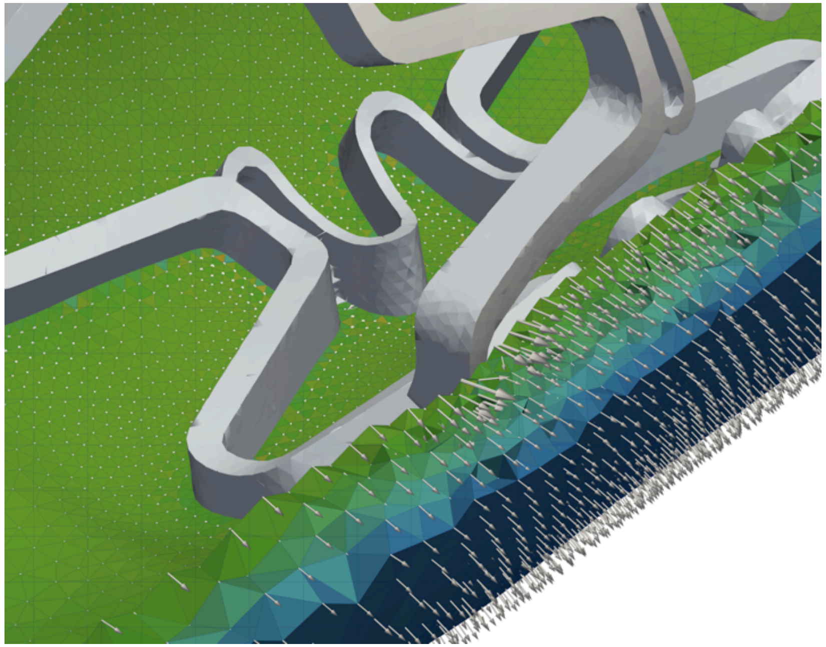

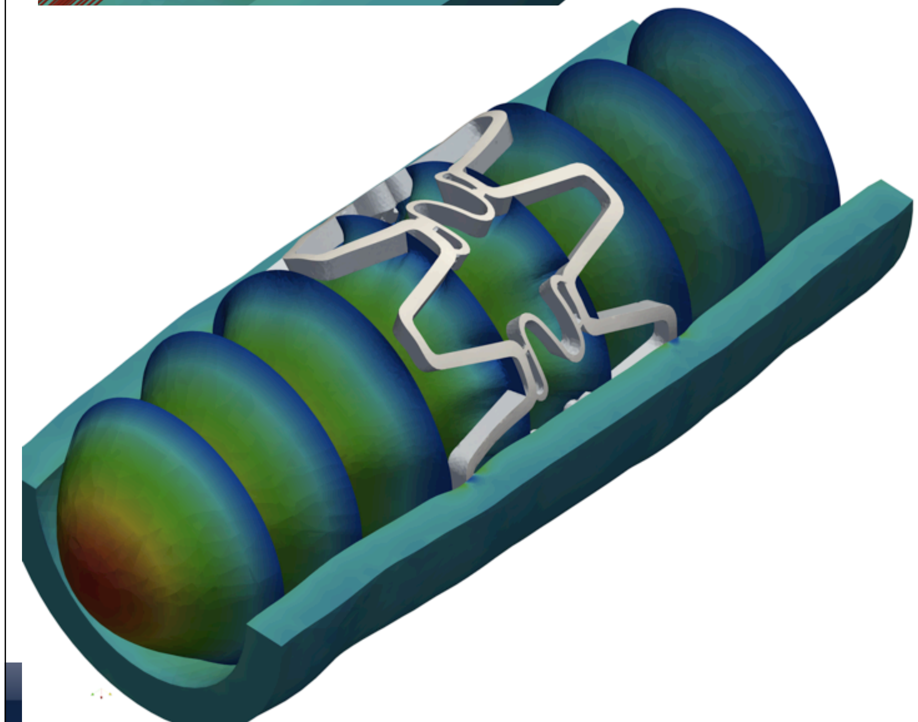

- Simulations by C.D'Angelo,
- P.Zunino, MOX - in collaboration
- with LABS, PoliMi

Isosurfaces of drug concentration (lumen)

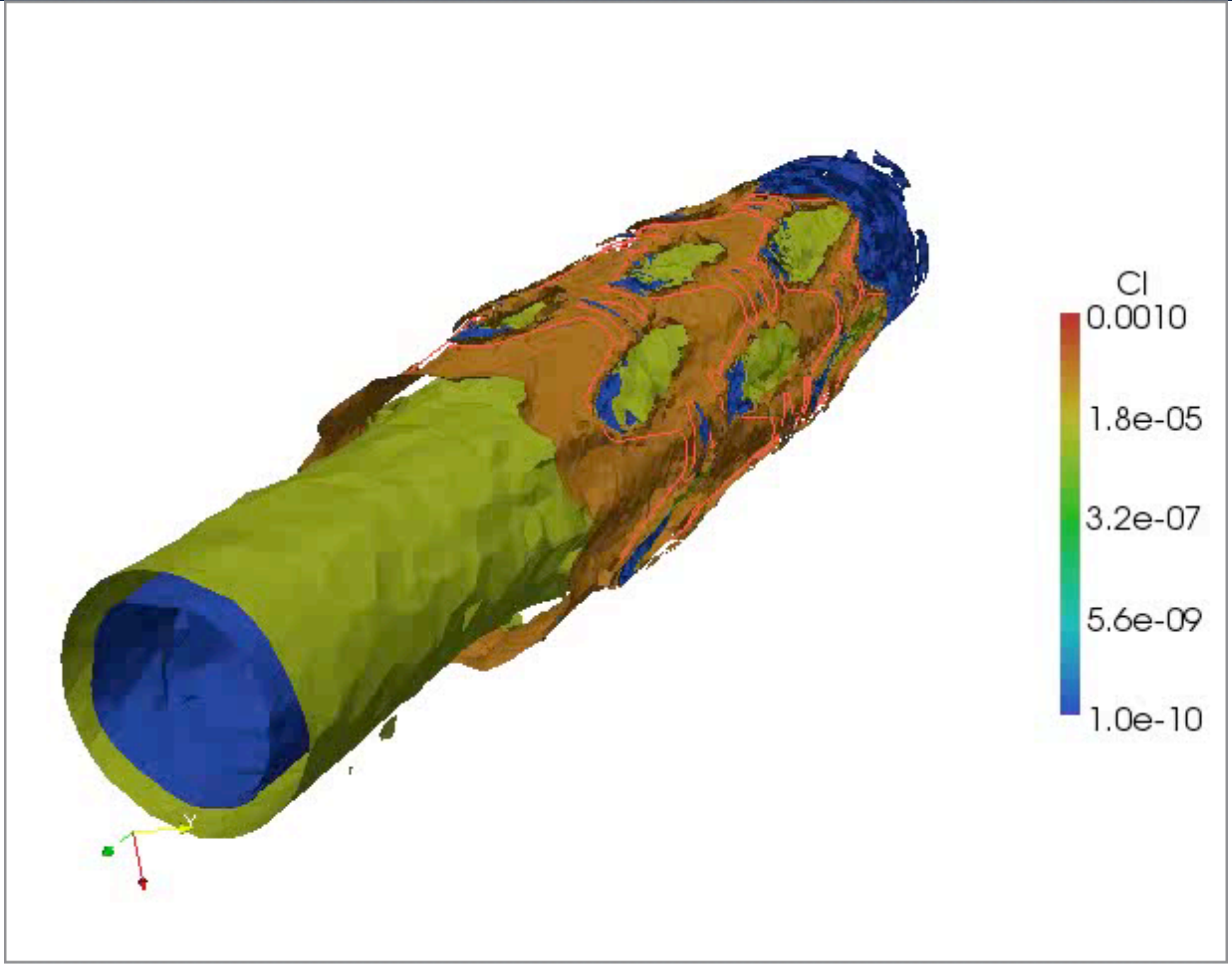

(C.D'Angelo,P.Zunino)

Isosurfaces of drug concentration (arterial wall)

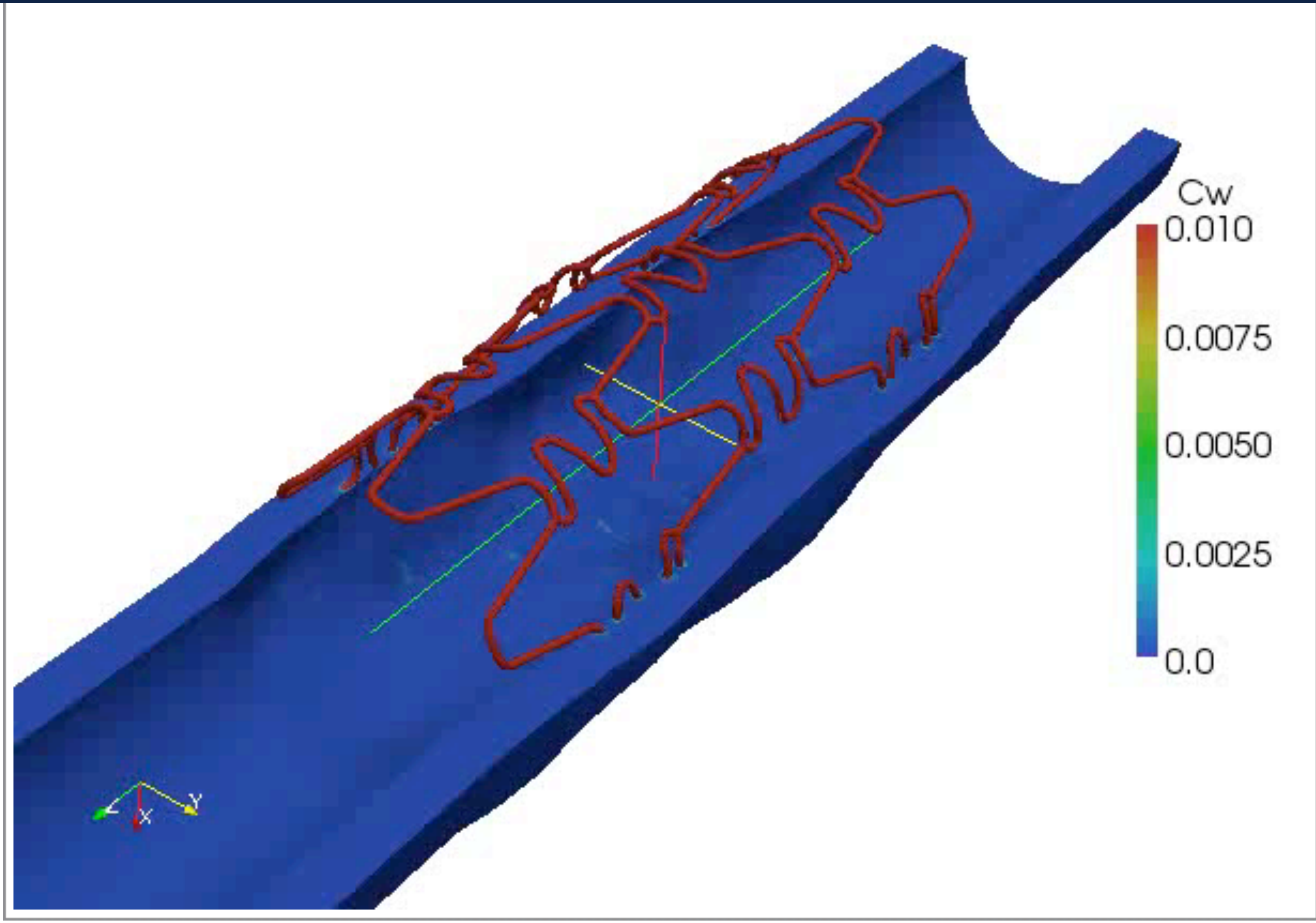

(C.D'Angelo,P.Zunino)